J. Membrane Biol. 76, 197–225 (1983)

The Journal of
Membrane Biology

Topical Review

Ionic Selectivity Revisited: The Role of Kinetic and Equilibrium Processes in Ion Permeation Through Channels

George Eisenman and Richard Horn
Department of Physiology and Brain Research Institute, ULCA Medical School, Los Angeles, California 90024

Key Words selectivity · channels · energy profile · rate theory · permeability · conductance · binding · barriers · sites · reversal potentials

Introduction

The intent of this paper is to bring up to date an earlier theory of *equilibrium* selectivity [23, 24], with emphasis on making it applicable to the permeation of membrane channels and carriers, which involve *kinetic* considerations [8, 56]. We will review critically and unify a number of conceptual advances that have occurred since 1961, particularly the recognition by Hille [56] of how the same energetic principles that describe equilibrium selectivity of binding sites also apply to the peaks of the energy barriers (the so-called selectivity filters) involved in the kinetics of permeation. In the process, the precision of the term *selectivity* will gradually be increased. We will start with the intuitively simple comparison of effects of one ion *versus* another. Then we will proceed through more theoretically based classical concepts such as permeability ratios, conductance ratios, and ratios of binding affinities, all of which can be interrelated quite directly in sufficiently simple channels. It will become clear that these concepts lose their crispness and usefulness in multi-barrier channels as a consequence of asymmetry and/or possible multiple occupancy. Our formulation is influenced by a number of useful concepts from classical rate theory [40, 48, 126, 128], where the channel is viewed as having a static energy profile for a given state of ion occupancy; but we will also consider the consequences of viewing the channel as a dynamic structure with a fluctuating energy profile [83, 85].

Besides presenting a topical review of selectivity, we have found it necessary to consider two subjects which are so new that they have received little attention as yet in a selectivity context. These are the effects in multi-barrier channels of *asymmetry* and *multiple occupancy*. This is because a number of classical concepts, and even ways of thinking about selectivity, are implicitly conditioned by conclusions that have been reached from considerations heretofore largely restricted to channels occupiable by no more than one ion at a time, or to channels with only one significantly rate determining barrier[1], or to channels which are symmetrical. To exemplify the effects of channel asymmetry, we examine in a simple two-barrier one-site model the consequences of asymmetry for reversal potential selectivity. To exemplify the effects of multiple rate-determining barriers, we also examine some implications of the energy profile which can be inferred for the gramicidin channel.

In the process of presenting this material, we describe certain relationships between selectivity as seen in different phenomena such as conductance, reversal potential, and binding – at least in systems which are simple enough for these classical concepts to retain their utility. This should lead to an understanding of why different measures of selectivity sometimes lead to different apparent selectivities, even in very simple channels. We also will define some guidelines for the applicability of these classical concepts and give some suggestions as to how to define selectivity when they fail, as fail they must, in those biological channels which are asymmetric and/or occupied by more than one ion at a time.

[1] Or the equivalent of a single barrier in a membrane of macroscopic thickness, namely a homogeneous Nernst-Planck diffusion regime.

Historical Development of Selectivity Concepts Used to Date

1. The Existence of Irregular Sequences for the Group Ia Cations and Qualitative Suggestions for Their Origin

The existence in biology and chemistry of effects for the group Ia cations (Li, Na, K, Rb, and Cs) following neither the simple sequence associated with naked ion size nor with the Hofmeister series of hydrated radii but in apparently quixotic irregular sequences was recognized for a long time (e.g., [61]; for an up-to-date compilation *see* [76]). In the chemical literature a number of suggestions were made to account for these which generally were based on concepts, natural to chemists, related to affinity or binding. The first was Jenny's [71] proposal that such sequences could be interpreted as various stages in a transition between limiting hydrated and dehydrated sequences where "the most hydrated ion will be the first affected by the dehydration process." The factors governing dehydration were unspecified until Bungenberg de Jong [12] suggested an atomic parameter, the polarizability of the interacting anion, as a possible cause for a series of "polarizability sequences," which he explicitly enumerated. These sequences, which are the ones implicitly required by the Jenny postulate, never have ions other than Li or Cs as the most preferred species and therefore did not correspond to the selectivities observed in biological phenomena, in which the K or Na preferences were noteworthy. Eisenman, starting from a large data base of aluminosilicate glass electrode selectivity in which preferences for K or Na were also prominent features [33], and recognizing the existence of a parallel selectivity in aluminosilicate ion exchanger minerals, postulated a fundamental similarity between the sites in aluminosilicates and in living cells and proposed that such selectivity sequences would be expected to occur from variation of the "electrostatic field strength" of an interacting anionic site (34; summarized in Mattock's text, [94], pp. 130–134). In contrast to Jenny, he proposed that the *least* strongly hydrated ion (i.e., the largest) would be the one to be *first* affected by the dehydration process but that with increasing dehydration the smallest ion would approach closest to the site and therefore interact most strongly. Although Eisenman's initial considerations were still intuitive, being couched in mechanical terms (e.g., effective ionic radius), and did not yet recognize that selectivity could be formulated more rigorously in *energetic* terms as the difference in Gibbs' free energy lost in dehydrating the ion and that gained by interaction with the binding site, they did generate the irregular selectivity sequences in an intuitively satisfying way, as is shown in the reproduction in Fig. 1 of the original field strength-ionic radius plot [34, 94].

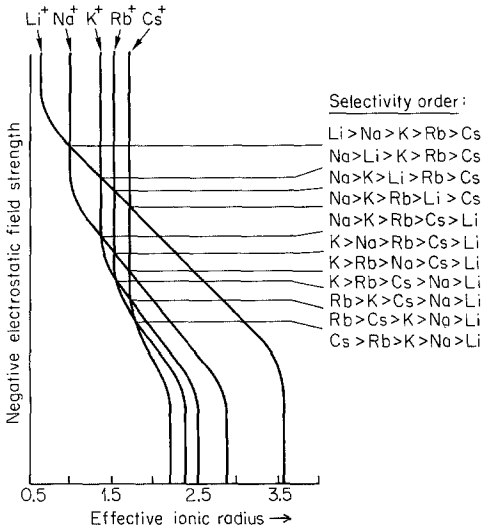

Fig. 1. Field strength *vs.* effective ionic radius. Described in text

The principle concepts of the existence of *selectivity sequences* and of a *pattern* of such sequences can be usefully appreciated even at the intuitive level of Fig. 1. Thus, the particular expectations of Fig. 1 are for 11 selectivity *sequences*, listed below, which occur in the following *pattern* with increasing negative electrostatic field strength of the interacting site.

Li > Na > K > Rb > Cs	Sequence	XI	(at highest field strength)
Na > Li > K > Rb > Cs	Sequence	X	
Na > K > Li > Rb > Cs	Sequence	IX	
Na > K > Rb > Li > Cs	Sequence	VIII	
Na > K > Rb > Cs > Li	Sequence	VII	
K > Na > Rb > Cs > Li	Sequence	VI	
K > Rb > Na > Cs > Li	Sequence	V	
K > Rb > Cs > Na > Li	Sequence	IV	
Rb > K > Cs > Na > Li	Sequence	III	
Rb > Cs > K > Na > Li	Sequence	II	
Cs > Rb > K > Na > Li	Sequence	I	(at lowest field strength)

Notice in these sequences that each alkali cation, in turn, is favored and moreover that a particular pattern of selectivity inversions occurs. These sequences were shown to have a wide natural occurence and were subsequently generated on a more quantitative basis from simple models for the relevant Gibbs' free energies of binding *vs.* hydration ([23]; *see also* [90], Fig. 4.9). Interestingly, these sequences, more commonly referred to as "Eisenman sequences," are the reverse of the polarizabil-

ity sequences of Bungenberg de Jong and Jenny, which can be obtained simply by reading these sequences from back to front (i.e., by replacing the symbol $>$ by $<$). The reasons for this will be discussed later under Topology, where we will show that the particular Eisenman sequences correspond to the situation where a selectivity optimum for each alkali cation occurs as a monotonic function of cationic size; whereas the polarizability sequences will be shown to correspond to a selectivity minimum for each cation.

Contemporaneously, in the physiological literature a more mechanical view of selectivity was also developing (for history *see* [56]) involving sieving by pores according to ion size, which was quite natural for physiologists impressed by osmosis, although concepts of affinity were also recognized [61, 108]. For example, sieving was emphasized by Michaelis [96], who proposed that cell membranes contained channels which distinguished between ions on the basis of "friction with the water envelope dragged along by the ion." Sieving concepts were extended by Boyle and Conway [9] and by Ling [89], who used hydrated radii to calculate the Na *vs.* K selectivity to be expected from the differences in electrostatic interactions at their distance of closest approach to an anionic site. Considerations based upon particular stable hydration states were further ingeniously developed by Mullins [100, 101] and by Lindley and Hoshiko [88]. Such mechanical theories can, at least in principle, be unified with affinity theories by specifying friction in terms of the activation energy of the transition states for migration.

2. The Quantitative Formulation of Selectivity Among Group Ia Cations as a Balance of Attractive Energies of Ions for Sites vs. Water

A major advance in selectivity theory was the recognition [23] that *equilibrium* selectivity among the group Ia cations could be rigorously formulated as a balance between the energies of ion-water *vs.* ion-site interactions which were calculated for a number of hypothetical situations in a variety of ways, all of which yielded the aforementioned set of 11 Eisenman sequences with only minor anomalies. The calculations (*see* [23] and [24]) included: (a) a purely heuristic electrostatic model for the competition between a single multipolar water molecule and a single monopolar site, (b) more physically realistic coulombic models for ion-site interactions in onefold and sixfold coordination states using experimentally known hydration energies, (c) halide models for sites using thermochemical data for the energies of ion-site interaction in various coordination states (ion pairs or crystal lattices) and for hydration energies, and (d) models using free-solution data for the effects of varying the degree of hydration, where the energies of a given hydration state were assessed from the known free energies of dilution for the halide salts. It should be pointed out that the 11 Eisenman sequences were also generated by Ling from a sophisticated analysis (including Coulomb, Born, Keesom, London energies) of a particulate linear array of ion, site, and water molecules in those situations where site polarizability was low (*cf.* [90], Fig. 4.9).

Note that the above modelling is of two types: highly oversimplified partial models which emphasize only the most important (e.g., coulomb) contributions to the energy and more complete models which make no such restrictions. In particular, Eisenman's, essentially thermochemical, models of types (c) and (d) are complete models insofar as they contain *all* the terms that contribute to the total energy, as do Ling's calculations for a linear array, although they apply to only approximately realistic situations. Partial coulomb models give some insight into the molecular forces involved; whereas the complete thermochemical models enable one to predict selectivity using tabulated values (heats and entropies of formation, activity coeffients, etc.) for the halide anions as prototypes for anionic groups more generally (a useful relationship between the field strengths of of halides and oxyanions, via the pK_a, has been given elsewhere [23, 27]).

The principle importance of this work is in its formulation of the problem of selectivity in terms of the Gibbs' free energy and in its removing the mystery of irregular sequences by its demonstration of how directly the classical attractive forces of chemistry lead to the observed selectivity sequences and their pattern. The electrostatic model calculations were subsequently extended to include dipolar (neutral) sites [26, 30, 77]; and thermochemical modelling of neutral sites was also carried out for peptide ligands using amide solvents as models [30, 77]. The Eisenman selectivity pattern was, somewhat surprisingly, found to hold even for uncharged dipolar ligands, a result which was rationalized from examination of the effects of interdipolar charge distribution and ligand coordination numbers ([26], Fig. 14).

Two conclusions reached by Eisenman in 1961 are worth noting: that "the primary physical variable controlling equilibrium cationic specificity is the field strength of the anion" (representable in

a coulomb model by an equivalent anionic radius, r_-) and that "the primary factor controlling the magnitude of selectivity among ions at a given field strength...is the amount of water admitted into the vicinity of the site". These simplifying concepts have proved useful in a variety of physical systems [19, 107, 116]. A recent example is Eberl's [21] use of both the equivalent anionic radius and the free solution model for water swelling to predict successfully the group Ia cation selectivity and interlayer water content in clays. From the relative insensitivity of the selectivity pattern to the details of coordination and hydration states, we can provisionally reach the following two conclusions. First, the pattern must reflect an underlying asymmetry at the molecular level in the ion-site *vs.* ion-water interaction energies. Second, the essence of this asymmetry is that *ion-site interaction energies fall off as a function of cation size as a lower power of the cation radius than do ion-water interaction energies.* This will be examined more fully in sections 4 and 5 below.

Although all the above models are explicit, quantitative, and unambiguous in their predictions, it must be emphasized that they do not purport to be *ab initio* calculations for any real molecular structure (except for crude calculations for the silicate and aluminosilicate binding sites of glass [24]). True *ab initio* calculations are just now beginning to be successfully carried out for typical carrier molecules by A. Pullman and her colleagues [52, 53].

3. Extension to Other Species

Halide Anions

As pointed out in [23, 24] the principles are of course the same as for the Group Ia cations; and anionic selectivity sequences and patterns of these have also been developed [19, 25, 27].

Monovalent Cations Other than Group Ia

Although we will not discuss the subject further here except by way of an example in Fig. 19 for the energy profile of the gramicidin channel, a discussion of selectivity would be incomplete if it did not mention that monoatomic monovalent cations other than those of group Ia, such as Tl, Ag, and H, can provide information as to ligand type and orientation of selectivity filters and binding sites, as can polyatomic ions such as NH_4 and its derivatives. Hille [54] clearly demonstrated that the Na Channel was substantially permeable to a variety of polyatomic cations and used these to obtain structural information about its selectivity filter, and Eisenman and Krasne [30] have continued this approach by developing a series of selectivity fingerprints for such species for a variety of ion binding molecules of known structure [30, 32, 77].

Divalent Cations

Truesdell and Christ [122] extended Eisenman's electrostatic models to the divalent cations of group IIa by assuming the substrate to contain either isolated pairs of sites of charge -1 or sites of charge -2 and showed that divalent cations were preferred over monovalents by -1 charged sites separated by less than 5Å. Eisenman [25] examined monovalent *vs.* divalent selectivity further using a thermochemical alkali halide crystal model, and also carried out calculations on simple coulomb models for the effects of allowing local departures from electroneutrality, so as to include the possibility of competition on a molar as well as an equivalent basis. Subsequently, Sherry [116] examined more refined models and achieved considerable success in accounting for the ion exchange properties for monovalent and divalent cations of zeolites.

The question of how a biological channel can be selective for divalent cations over monovalent cations is intriguing, particularly in the absence of any known artificial channel showing such behavior. The general question of monovalent *vs.* divalent selectivity has been examined by Simon and Morf ([118], *see also* [99]), in the course of treating the ion selectivity of cyclic carriers. They examined theoretically a number of important factors involved in divalent *vs.* monovalent discrimination which are also pertinent to channels. While it is difficult to transfer directly to channels in a (low dielectric) lipid membrane their conclusions for the stability of complexes with carrier molecules in polar solvents, their identification of the role played by the overall dimensions of the complex is of interest.[2]

Even through a narrow channel there need be no difficulty in sufficiently rapid flux of ions provided a stepwise replacement of water molecules by ligands could occur analogous to that known to occur for monovalent cations [22]. It is even

[2] In defining monovalent *vs.* divalent selectivity it is important to realize that, owing to the different valencies, the relative effectiveness of divalent cations must, in a system obeying electro-neutrality, increase with dilution (since the relative contributions of the monovalent cation to the potential has twice the power dependence on concentration as does that of the divalent cation). This is not obvious from the form of the equation used by Lewis [87] but is easily seen in Truesdell and Christ's [122] Eq. (11.10) or in Morf's [99] Eq. (6.10).

possible for a long tubular channel to provide an appropriate energy profile for rapid divalent permeation through counterbalancing the unfavorable image energy with a sufficiently favorable ligand interaction energy.

4. Topology of Selectivity Sequences

The most striking feature of experimentally observed selectivity is its unique dependence on ionic size, which for Eisenman sequences can show a pronounced optimum for an intermediate sized species (e.g., K or Na) while simultaneously disfavoring larger and smaller sized ions. This is illustrated in Figs. 2 and 3 for a variety of experimental data by plotting selectivity (increasing selectivity upwards) as a function of the reciprocal of the naked cation radius.

Figure 2, after Grell et al. [51], illustrates the selectivity optima for Rb, K, and Na (indicated by arrows) seen in complexation in methanol for a number of well-known complexing agents. Figure 3, after Eisenman and Krasne [30] shows similar optima for Rb, K, Na, and Li, respectively, for valinomycin, the K channel, the Na channel, and the enzyme adenylate deaminase. For the first three systems permeability ratio selectivity is plotted; while for the fourth Michaelis-Menten binding selectivity is plotted.

The existence of selectivity optima like those in Figs. 2 and 3 to intermediate sized ions is an implicit property of the Eisenman sequences, which can be shown explicitly by replotting selectivity as a function of reciprocal cation radius, as has been done in Fig. 4. This figure illustrates the topology of the Eisenman sequences. Again, increasing selectivity is plotted upwards. Here the continuous curves separate regions in which the sequences indicated by the appropriate Roman numerals prevail. Note that the curves are not drawn to any particular equation but merely delimit the space in a way compatible with the topology. Each curve describes the selectivity of one given system. For example, the curve between regions *II* and *III* corresponds to the selectivity sequence Rb > Cs = K > Na > Li, which separates sequence *II* (Rb > Cs > K > Na > Li) from sequence III (Rb > K > Cs > Na > Li). A system obeying sequence *III* would be described by a curve having the same general shape as the curves drawn in the figure and lying in the region labeled *III*.

It is a characteristic of such a plot that an Eisenman selectivity sequence always appears as an upwardly *convex*, essentially monotonic, uninflected curve having a single *maximum*, which can

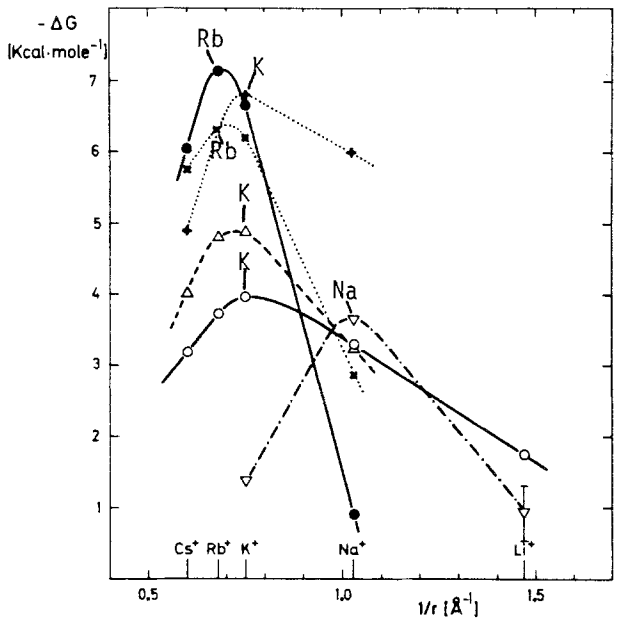

Fig. 2. Specificity of alkali cation complexing agents (after [51]). Free energies of complex formation in methanol at 25 °C *vs.* reciprocal cation radius. The selectivity optima are shown by arrows for each of the indicated cations for the following molecules: Valinomycin (filled circle); enniatin B (open circle); nonactin (triangle); antamanide (inverted triangle); dibenzo-30-crown-10 (x); dibenzo-18-crown-6 (+)

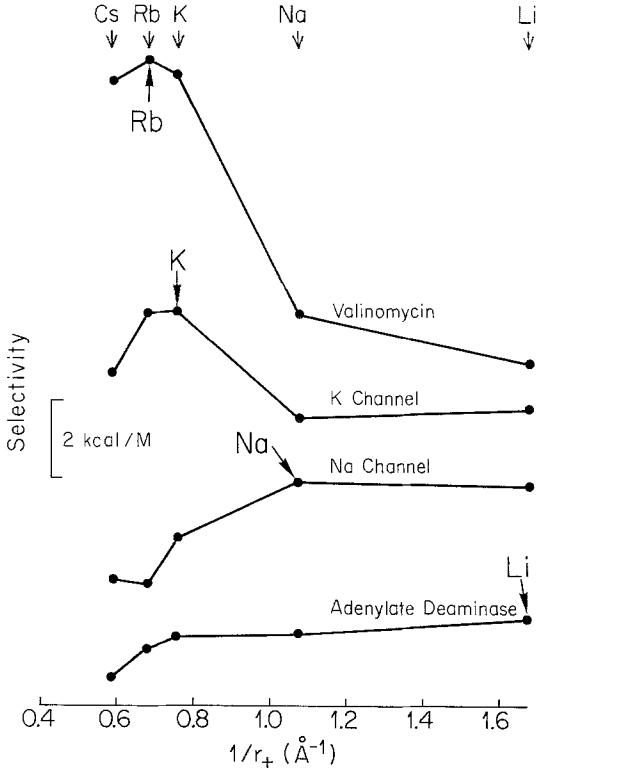

Fig. 3. Selectivity optima for Rb, K, Na and Li for a carrier, two channels, and an enzyme. The optima are indicated by arrows (the locations of the reciprocal radii for Cs, Rb, K, Na and Li are shown above). (Described in text.) Note that the K channel data suggest a Li anomaly, discussed in Fig. 5

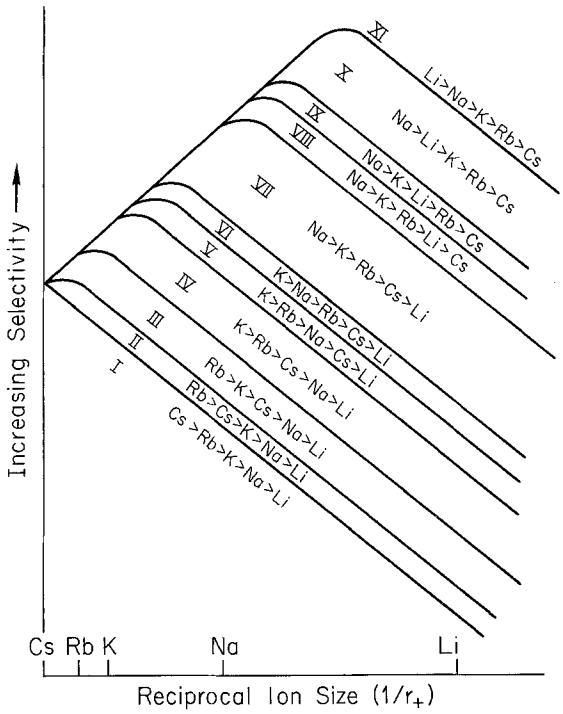

Fig. 4. Topology of Eisenman sequences. (Described in text)

occur at a radius corresponding to any one of the group Ia cations. This maximum corresponds to a selectivity optimum. In contrast, on such a plot the polarizability sequences would be described by upwardly *concave* curves having a single *minimum*; so that only Li or Cs can be the most preferred cation; and the intermediate sized cations are always disfavored. This topology corresponds to reading Fig. 4 with increasing selectivity downwards.

Usefulness

Such a plot of selectivity against reciprocal cation radius is very useful because it makes it possible to diagnose whether one is dealing with an Eisenman sequence or a polarizability sequence, or a deviant from one of these, without having to remember the particular sequences. For on such a plot an anomaly in an Eisenman sequence appears as an additional optimum or, when less severe, as an inflection, as exemplified in Figs. 5–7.

Figure 5 plots the permeability ratios tabulated by Gorman et al. [50] for a variety of K-channels; and from the shape of the plot it is immediately apparent that an Eisenman sequence with a "Li anomaly" (*cf.* [109]) is being observed because, except for Li, the curve is convex upwards. The tendency to such an anomaly is even apparent in the nondeviant Eisenman sequence IV found by Gay and Stanfield [47] for the skeletel muscle channel.[3] From the way Fig. 5 has been plotted it is also apparent that the selectivity for all K channels are fundamentally the same, whether or not their sequences actually show a Li anomaly.

Figure 6 plots the *binding affinities* (as the logarithm of the reciprocal of the dissociation constant) for group Ia cations as measured by Hille and his colleagues [2] for the endplate channel, whose affinity sequence (Li > Cs > Rb > K > Na) would seem to show a marked Li anomaly in relation to an Eisenman sequence. However, from the upwards concavity of this plot we can now diagnose that these ions are actually following a pure polarizability sequence. It is curious, and intriguing, that the sequence of *permeability ratios* from (reversal potentials) for divalent cations (Mg > Ca > Ba > Sr) in this channel, noted by these authors as "not even one of the Eisenman sequences," can also be seen from the plot of Fig. 7 to follow a polarizability topology. It is also worth noting that the *permeability ratios* for alkali metal cations conform to sequence I [1], an illustration of the common finding that selectivity for binding and permeability do not in general agree for reasons discussed in the section "Relation of conductance ratios to permeability ratios and binding constants."

[3] Although Reuter and Stevens have suggested non-coulomb (e.g., higher) terms in their power series representation of selectivity as the cause of their observed deviation from a pure coulomb expectation and such effects can account for the data to be described in Figs. 6 and 7, one must be alert to the possibility that such deviations could occur from alternative causes, e.g., as a trivial consequence of an asymmetry of a multi-barrier channel, or as a consequence of multiple occupancy.

It should be noted that Li anomalies have also been previously observed for glass electrodes (Eisenman's [24] order VIIa is one example) and have been suggested also to be a feature of the biological selectivity pattern ([25], Fig. 9). They have a natural basis in the expected polarizing power of the small Li ion, which causes noncoulomb terms to contribute more to the energies of interaction of this ion with polarizable ligands than for the larger cations. Such Li anomalies can be seen in Ling's calculations for the effects of polarizability in a one-dimensional model ([90], Figs. 4.9–4.11); and, indeed, a relatively minor alteration in the Li isotherm in Fig. 1 (displacing its diagonal segment downward and slightly to the left, as would be expected for a polarizability contribution) suffices to represent all biological and glass electrode selectivities known to date. Note also that energetic contributions favoring smaller ions which behave formally like polarizability need not be due to electron cloud deformations of individual atoms but can also occur as a group polarizability by way of a rearrangeability of the multiple ligand groups usually involved in a site or barrier. S. Krasne (*personal communication*) has even shown in model calculations that repulsive (electrostatic) ligand-ligand interactions can actually generate the 11 polarizability sequences at extremely high ligand field strength as a subsequent set beyond the usual 11 Eisenman sequences.

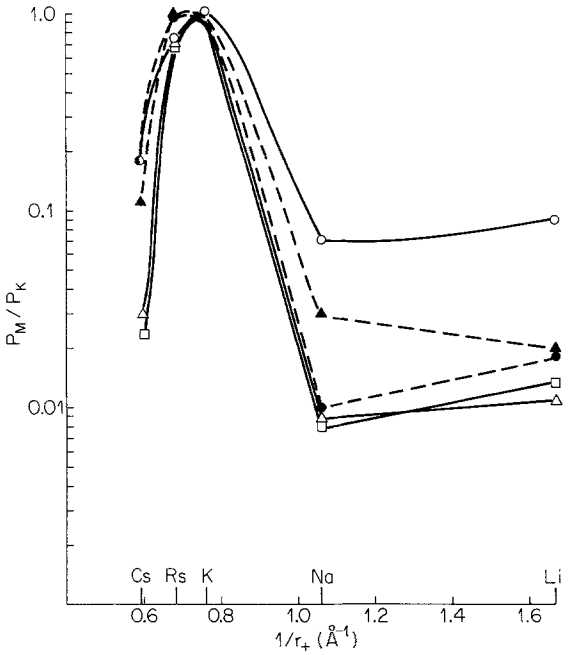

Fig. 5. Topology of selectivity for the K channel. The logarithm of permeability ratios for a variety of K channels (after data of Table 1 of [50]) is plotted *vs.* reciprocal cation radius. Delayed K current, *Helix* neurons (open circles, [109]); delayed K current, skeletel muscle (filled triangles, [47]); delayed K current myelinated axon (filled circles [55*a*]); light-dependent K current, scallop distal photoreceptors (triangles, [50]); Ca-activated K current, *Aplysia* neurons (squares, [50]). Note the similarity in the overall topology and the tendency toward a Li anomaly even in the data of Gay and Stanfield (filled triangle) which obey a regular Eisenman sequence

5. Differences Between Interaction Energies with Water and with Ligands as the Basis for Patterns

In the preceding sections we have merely demonstrated the existence of selectivity optima (or minima) and shown how these can be described through various selectivity patterns. Here we turn to some general considerations in order to make two points. First, we describe how such optima can arise from underlying interactions which are themselves monotonically increasing functions of decreasing ionic size. (In the process, we show how the energies underlying Eisenman-type, polarizability-type, and anomalous-type sequences differ). Then, we discuss the two principle factors which contribute to selectivity; (i) the electronic structure (e.g., "field strength") of the individual ligands making up a binding site (or selectivity filter) and (ii) structural constraints on the array of the ligands comprising the site (or filter). Selectivity filter is a term used to describe the selectivity at an energy maximum in contrast to that at an energy minimum.

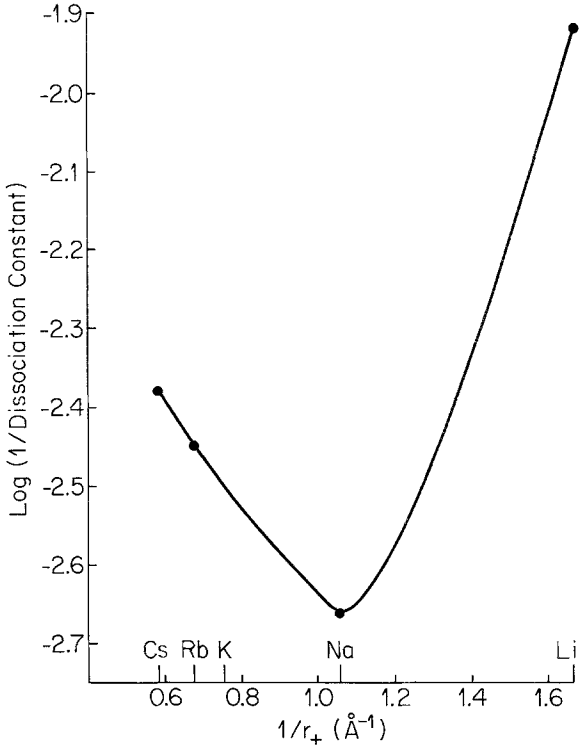

Fig. 6. Topology of binding affinities of the endplate channel for group Ia cations, as measured in [1]. Note the polarizability topology. (Described in text)

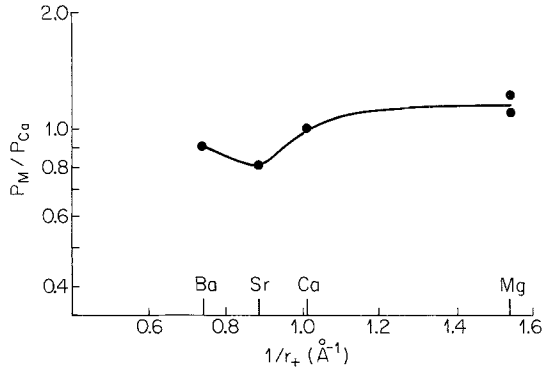

Fig. 7. Topology of permeability ratios for divalent cations measured from reversal potentials [1]. Note the polarizability topology. (Described in text)

Interaction with the selectivity filters and binding sites of a channel almost certainly involves the replacement of one or more water molecules by ligands belonging to the channel protein (e.g., carbonyls). All energetically based selectivity theories formulated to date [22, 23, 30, 77, 109, 118] agree that underlying the observed selectivity optima is a competition between energies (hydration *vs.* ligand interaction) which are themselves *continuously increasing functions of decreasing ion size.* The kernel of selectivity theory, whether applied to equilibrium free energies (e.g., of binding sites)

or activation free energies of transition states (e.g., of selectivity filters), is the explanation of how a selectivity optimum can occur from underlying interaction energies (with water on the one hand and with the channel ligands on the other) which are themselves continuously increasing functions of decreasing ion size.[4]

For concreteness, let us discuss the selectivity seen in the binding of a monovalent cation to a site in a channel. How binding energy differences, which are themselves monotonic, can lead to a selectivity optimum for the relative affinities has been discussed extensively elsewhere [30, 77] and can be illustrated with the aid of Fig. 8. Figure 8 schematizes the dependence of free energy on the reciprocal of the naked cation radius for a variety of situations. The hydration energy is shown by a dashed curve; while that for binding is shown by a solid curve. All energies are referred to vacuum and relative to Cs, and will, accordingly, be designated as relative energies for brevity in the following discussion because they are always taken relative to the reference cation, Cs. Selectivity is, of course, defined by the difference between the energies of the solid and dashed curves. From top to bottom four types of selectivity situations are indicated: "proportional," "Eisenman," "polarizability," and "Li anomaly."

We discuss binding here, but similar reasoning can also be used for the comparison between peak energies underlying permeability selectivity. The roles played by binding energies, as well as peak energies, in variously defined selectivity phenomena will be clarified in a later section, where the different phenomena will be interrelated in terms of the underlying energy profiles.

The situation labeled "proportional" refers to one in which the relative binding energies for the cations (solid curves) have the same shape as the relative hydration energies (dashed curves); that

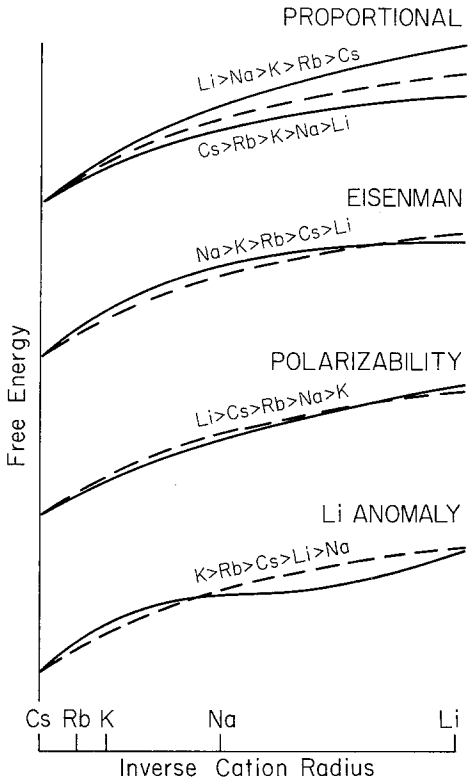

Fig. 8. Energies underlying four different selectivity topologies. (Described in text)

is, relative binding is simply proportional to relative hydration, being merely larger or smaller. The selectivity in this situation will then show no optimum but be either in one extreme sequence Li > Na > K > Rb > Cs or the other Cs > Rb > K > Na > Li, as labeled. We will call such behavior proportional (it has previously been termed symmetrical [30, 77], but we replace this term to forestall confusion with asymmetric channels). These references should be consulted for further details.

Note that the energy curves for binding and hydration can be represented by suitable power series of the inverse cation radii, so that proportional curves have coefficients that are the same as those that describe the hydration energy, but where all terms higher than the zeroth power are multiplied by a constant. Nonproportional curves (previously called asymmetrical [30, 77]) do not satisfy this condition. Eisenman sequences are generated by binding energies where lower power terms dominate for binding compared to hydration; polarizability sequences are generated by binding energies where higher power terms dominate for the site (*cf.* [109]).

The other situations in Fig. 8 correspond to various types of nonproportional relative binding energies. Thus, the shapes of binding energy curves

[4] It should be noted that there are secondary, presumably smaller, contributions to the free energy which are not expected to be strictly monotonic functions of ion size: for example, entropic effects (*cf.* relative hydration enthalpies *vs.* free energies in Fig. 51 of [77]), as well as energy changes due to exchanging water molecules between the channel and bulk water, as well as due to conformational changes in the channel. It is also important to realize that even at the top of an energy barrier in a channel (which is, of course, a less favorable situation than in a binding site) the free energy of an ion has been lowered relative to vacuum considerably by favorable interactions with the polar material of the channel. This is the catalytic effect of the channel as a permease. Indeed, if the least favorable interactions of the permeant entity (the ion plus any associated water molecules) with the channel's polar groups do not bring the permeant species to within about 5 kT units (6.7 kCal) of its energy in water, permeation will occur too slowly to be easily measured at the single-channel level.

that underly the Eisenman sequences, the polarizability sequences, and sequences with a Li anomaly are indicated in the subfigures, with the selectivity sequences corresponding to each curve being labeled. (The curvatures have been exaggerated for emphasis; Fig. 2.2 of [30] should be consulted for more realistic curves.) Note that the binding energy underlying an Eisenman sequence is more curved than the hydration energy, whereas for a polarizability sequence it is less curved. (This is not in conflict with the statements in the preceding paragraph about the size dependences on various power terms; energy is being plotted against the *inverse* of the cation size, so that a lesser curvature than water means a relatively greater binding than hydration energy for the smaller than for the larger ions.)

Two classes of theories have been proposed as to how nonproportional interaction energies can arise. One class [23, 90] emphasizes the nonproportionality expected in the interactions between cations and individual ligand groups making up a binding site, and neglects steric constraints on the array of ligands. The other class [22, 118] starts with the implicit assumption that the individual ligand groups have energies proportional to water molecules and then assigns the nonproportionality to steric constraints on the array of ligands. In general both factors are likely to be involved; but situations in which these various sources of nonproportionality are thought to prevail have been enumerated elsewhere [22, 30, 32, 76, 78, 118].

Extension of Selectivity Theory to Kinetic Phenomena in Open Channels

Although measurements of simple equilibrium binding affinities for channel sites can sometimes be carried out, especially in the case of channel blockers, ion selectivity in membrane permeation is usually inferred from two kinds of electrical measurements: (i) *reversal potentials* and (ii) *conductance measurements* for comparable concentrations of permeant species. Studies on model systems, as well as theoretical considerations, indicate that even these, most direct of electrical measurements, are strictly equivalent to each other only under restricted circumstances (*cf.* [38, 56]). However, as discussed below, they are relatable to each other, and to binding affinity as well, in terms of the energy profile they imply. For example, in sufficiently simple situations (e.g., a symmetrical channel occupied by at most one cation at a time), these measurements can be interrelated quite directly. Since electrical measurements involve kinetic contributions to the permeation process, their explanation cannot be expected to be given rigorously in terms of the equilibrium energetic concepts used to this point. The way to extend equilibrium selectivity considerations so as to apply rigorously to channel permeation has been proposed by Hille [56], using the concepts of Eyring Rate Theory [40, 128]. We believe that Hille's suggestion is not restricted to Rate Theory formulations (which strictly do not allow for individual barriers to have any shape, *see* later) and suggest that it is applicable to continuous energy profiles, such as we will drawn in Fig. 9, as well. Before discussing this further let us describe the hypothetical energy profile that an ion experiences in a channel.

1. The Energy Profile

In attempting to understand the movement of ions through channels it is useful to realize that an ion encounters energetic maxima (barriers) and minima (wells) in its journey from one side of the membrane to the other. For the moment we will consider the channel to be a structure in which the energy profile for a given occupancy state is attained instantaneously (i.e., the channel can rearrange its conformation rapidly enough relative to the time of passage of an ion to represent an equilibrium energetic situation). In this view the energy profile could be regarded as being static and time-independent for a given occupancy state. Later we will clarify this point and discuss implications of the channel as a dynamic (i.e., fluctuating) structure which may be affected by the movement of ions through it.

Figure 9 illustrates schematically an hypothetical free energy profile encountered by two different ions in traversing a channel. We have used a continuum representation here, signified by the smooth curves. For simplicity, the profile is given for equal concentrations of the particular ion, and with no imposed voltage, across the membrane. Each profile can be seen to be composed of several local maxima and minima, representing energetically less favorable and more favorable locations for the permeant ions. We will sometimes talk about such profiles in an Eyring rate theory approximation, in which case the local maxima and minima are not smooth curves but actually should be represented by sharp impulses.

The reference level (i.e., the zero level) is the free energy of hydration of the ions in the solution on each side of the membrane. By convention the profile is plotted, not as a function of ion location in the channel, but as a function of fractional elec-

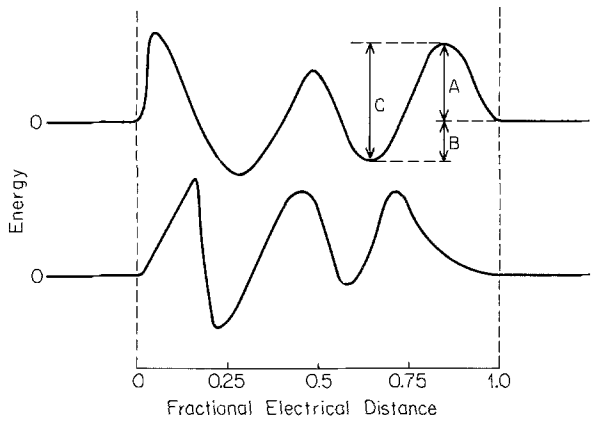

Fig. 9. Hypothetical Free Energy profile for two different ions in traversing a channel. (Described in text)

trical distance. If the electric field falls linearly across the membrane (which is unlikely), this plot will be equivalent to a plot of free energy as a function of position (*cf.* [68, 97]). Such a profile (if sufficiently detailed for all occupancy states of the channel) should be a completely general way of representing permeation for a single ion. This postulate is based upon the reasonable assumption that all aspects of permeation through such a channel can, at least in principle, be expressed in terms of the energy levels of these local energy minima and maxima, relative to the levels of the ions in water, the reference state for all biological permeation processes. Why this is so we hope will become apparent as we proceed.

A number of important concepts can be defined and clarified from this figure. First, the peak height, well depth, and barrier height are defined by the energies labelled A, B, and C for the adjoining maximum and minimum at the top right. The peak height (A) is the free energy relative to the standard free energy in the aqueous solution reference state. Similarly, the well depth (B) is the free energy of the minimum relative to aqueous. An ion moving out of this well to the right must scale an energy barrier with barrier height (C); whereas an ion moving into the channel from the right sees a barrier having the same height (A) as the peak. Note that it is only necessary to define two of these three quantities to define the other uniquely. Although it is usual to define kinetics in terms of the rate constants (i.e., in terms of the barrier heights) for the appropriate steps (e.g., [123]), from the point of view of selectivity it is the peaks and wells that are the most pertinent.

Asymmetric barriers are exemplified by the two different shapes of the left-hand barriers which are drawn to show a low voltage dependence across this barrier for entry and a high voltage dependence for exit for the upper ion and the opposite situation for the lower ion.

In terms of Rate Theory the energy maxima in Fig. 9 represent the energies of transition states. Diffusion past these unfavorable loci can be represented by single jumps over the corresponding barriers, progress over each barrier being proportional to the number of ions attaining the energy needed to surmount the activation energy to cross the barrier. The rate constant k_i for crossing over a barrier is related to the standard Gibbs free energy of activation G_i^* by

$$k_i = A_i \exp(-G_i^*/RT) \tag{1}$$

Where A_i is the frequency of attempted hops (between 10^{10} and 10^{13} sec^{-1}, depending on assumptions[5]) and RT is 592.2 Cal at 25 °C. The selectivity of these states can be inferred by applying to their energy levels the same principles previously developed for equilibrium selectivity.

2. Selectivity and the Energy Profile

The questions that become crucial to selectivity in a channel are: (i) How many barriers are there? (ii) What are their individual selectivities (i.e., what are the energy differences for different ions)? (iii) Where are they located in the potential field? Answering these questions is sufficient for a complete characterization of reversal potential selectivity for a channel that never contains more than one ion at a time. However, if one is interested in selectivity for a channel containing several ions simultaneously, or in selectivity measured at nonzero current even in the case restricted to one-ion occupancy, as in conductance selectivity, then similar questions have also to be answered for the wells. Additionally, for a multi-ion channel one also has to ask: (iv) How do the barriers and wells shift with loading the various species? And it is also useful

[5] A word about maximum limiting rates is in order here. Sometimes the rate of diffusion in a free aqueous system is taken as a limit for a channel; but a moment of thought will show that this is not a fundamental upper limit since it represents the diffusion of an ion accompanied by an hydration shell as well as a counterion cloud. For example, under sufficiently high force fields the ions can be stripped away from their accompanying ion clouds (the well known Wien effect). It is even conceivable that ions can be stripped away from their accompanying waters under appropriate conditions so that the true ("superconductivity") upper limit should be give solely by the mass of the ion. (The condition for such a high rate to be achieved is that a suitably uniform energy surface be provided by ligands whose interactions with the ion are comparable to the energies of interaction with individual water molecules.) Note that the absolute level of the energies is irrelevant; it is only the energy differences between most favorable and less favorable locations that matter.

to distinguish whether the effects of varying ionic concentrations follow merely as a consequence of their effects on membrane potential (e.g., reversal potential) or whether they are due to additional specific effects (e.g., repulsions, conformational changes, etc.).

Besides the above descriptive questions there are interesting theoretical questions to be answered such as: what is the molecular origin of the experimentally observed energy levels, and what molecular interactions are implied by the shifts of these levels with multiple occupancy?

Without in any way restricting considerations to Rate Theory, we will now use certain concepts from it to illustrate how the fundamental definitions of selectivity can be formulated in terms of the energy profile. It should be noted that for situations where the energy barrier fluctuates slowly on a time scale compared to the jumping rate, it may be necessary to use a more elaborate theory (*see* below).[6]

The selectivity of local minima in the energy profile can be understood quite simply. These favorable locations represent binding sites, whose selectivity can be assessed directly in terms of the Gibbs free energy of these levels, relative to water, using classical [23–25] selectivity theory.

The effects of local maxima (i.e., peaks) requires more explanation. The pertinence of these to selectivity follows from the insight of Hille [56], who recognized that the principles of Eisenman's equilibrium selectivity theory could be applied to these maxima. He pointed out that the interaction between an ion and a peak could be represented as a quasi-equilibrium condition, in accordance with the energetic approach of Rate Theory. Thus all that is required in extending the theory of selectivity to permeation is to apply the considerations of the previous sections to the Free Energy of *activation* instead of to the Free Energy of *binding*. At first it may not be clear why the energy at a peak in an energy profile should be given by the same general considerations as the energy at a well; but on reflection the reason is apparent. It is because the peaks represent only slightly less favorable interactions than those seen for binding. This is because for permeation to occur at a reasonable rate there can be no barriers higher than 5 kT, which means that for any highly selective channel of biological interest (where water molecules are replaced by ligands from the channel) favorable interactions must be supplied by the channel ligands to within 5 kT of the Hydration energy. Thus even the unfavorable locations of ions within a channel must be energetically the result of favorable interactions (compared to vacuum). This is the basis for the catalytic role of a channel as a permease[7]. In this view, the energy minima represent optimal coordination states, while the energy maxima represent slightly less optimal, but still necessarily favorable coordination states. If they were not based on largely favorable interactions, the ion would have to be desolvated without a replacement energy for the water molecules lost, which would cause the activation energy of the process to become so high that the process would occur at too slow a rate to be of interest. The molecular aspects of ion interactions with peaks and wells may differ, however, as we discuss under "Dynamic View of the Open Channel."

Hille in his "peak offset energy" concept [56] also proposed a particular pertinence to selectivity of the energy differences between the peaks; but the purity of this concept is lost in channels that can be occupied by more than one ion at a time [74].

3. How the Energy Profile is Characterized

Although not immediately relevant to selectivity *per se*, it is worth mentioning the principle experimental tools used to characterize the energy profile for a single ion. The most direct method is the measurement of the open channel current-voltage ($I-V$) relationship in the presence of identical concentrations of that ion on both sides of the membrane [70]. This relationship provides information about barrier height and location at low ion concentration, and about energy levels of both barriers and wells at higher concentrations. For example, at low concentrations of symmetrical electrolytes an outwardly rectifying $I-V$ reationship (i.e., larger conductance at positive than negative potentials) signifies that energy barriers are higher on

[6] A word on other complexities, such as the problems posed by the coupling of ion and water flows [41] is in order. These raise serious difficulties for any considerations of the present type which do not treat water molecules explicitly as molecular entities; but we believe it would be retrograde to revert entirely to a more mechanical (sieving) approach to selectivity in place of energetics.

[7] The behavior of conductance has a direct analogy with that for the rate of an enzymatic reaction (*see* [56, 81]), with the affinity being the reciprocal of the Michaelis-Menten dissociation constant and the maximal limiting conductance being the equivalent of the maximal limiting rate. The peak energy for the empty channel is inversely related to the product of affinity and mobility and can loosely be called the permeability being equal to the conductance in the limit of low permeant ion concentration (the X-intercept on an Eadie-Hofstee type plot [38]). For a discussion of channels functioning as enzymes catalyzing ion transport *see* Latorre and Miller [80].

the outer (i.e. extracellular) side of the membrane. In symmetrical systems (e.g., symmetrical bilayers with gramicidin channels or artificial carriers) an hyperbolic (i.e., supralinear) $I-V$ shape implies that a barrier deep within the membrane is rate determining, whereas a saturating (i.e., sublinear) $I-V$ shape signifies that the barriers at the surface are more important (*cf.* [29, 79, 81, 123]).

Another tool is the use of ionic channel blockers, which provide detailed information about the electrical location of wells, the relative heights of various barriers, and the shapes of barriers from the voltage dependences of blocking and unblocking rate constants [3, 16, 66, 67, 97, 98, 103, 127]. These experimental tools, although very important in determining the energy profile, are less relevant in our discussion of selectivity, and we will discuss them no further.

To decide the occupancy of a channel it is generally necessary to carry out other studies measuring permeation besides reversal potentials. Measurements of membrane conductances at zero current or characterization of the current-voltage characteristic, both carried out as a function of concentration, often suffice, the latter being useful also to assess where in the potential field the various barriers and wells are located. Flux coupling studies are also sometimes needed. The studies in well-characterized model channels, of which Gramicidin A is the outstanding example, provide useful prototypes for this (*cf.* [35, 36, 41, 123]).

4. Assumptions Contained in Rate Theory Representation of the Energy Profile

Rate Theory describes any process from diffusion to chemical reaction in terms of elementary jumps over energy barriers and can be used to represent the process of permeation in as much detail or with as much accuracy as desired. Classical Rate Theory describes nonequilibrium phenomena using equilibrium properties of the system, an approach which is valid provided the time needed for the adjustment of ligands after an ion jump is small compared to the dwelling time in the potential well [85]. This means that channels exhibiting slow conformational transitions relative to ion dwell times cannot strictly be handled by classical Rate Theory, but may require molecular dynamics methods (e.g., [44]).

In relation to alternative continuum (e.g., Nernst-Planck) formulations, inherent limitations of the Rate Theory approach have to do only with the graininess of description since they relate to the sharpness of the barriers and the consequent length of time spent in crossing them. As pointed out by Levitt [86] Nernst-Planck formulations allow for continuous displacement of an ion under the influence of the various forces whereas the Rate Theory approach represents a limiting case of the continuum approach where the energy barrier is so steep that the kinetics become dominated by the energy at the peak. The choice of formulation can be reduced to a matter of taste, since in principle any differences between the two approaches can always be removed by proliferating the number of barriers in the Rate Theory model (*cf.* [13]).

A further problem is that of using the simplification, common in most Rate Theory models, that an ion takes only a few hops to tranverse a channel of at least 25 Å in length. It seems more likely that many hops are needed to cover this distance. It can be shown, however, that a Rate Theory analysis can still be appropriate in this case; but the apparent energy levels of the barriers will be overestimated [68].

5. Transport Rate and Selectivity

A simplistic view of an ionic channel predicts that conductance should vary inversely with selectivity, as if the bigger the hole, the larger the conductance, and the less an ion will interact with the walls of the channel. In this view a high-conductance channel should have low selectivity and would tend not to discriminate between different ion species. To some extent this intuition is borne out by fact. For example, the classical, voltage-activated K channel of nerve has a relatively low single-channel conductance [5] accompanying its high selectivity; whereas the acetylcholine-receptor channel is both less selective and has a higher conductance than the K channel. Furthermore, larger ions can squeeze through the relatively nonselective acetylcholine-receptor channel [20, 69]. However, notable exceptions to this qualitative relationship have recently been reported. The calcium-activated K channel in tissue-cultured cells has a very large conductance (>100 pS), and is very selective for K over other monovalent cations [93, 104]. But another calcium activated channel [15] has a low conductance (<30 pS) and is relatively nonselective among the akali metal cations. The K channel reconstituted from sarcoplasmic recticulum (SR) is another example of a channel with both high permeation rates and high selectivity [17]. In order to explain these experimental observations, one has to imagine that the calcium-activated K channel and the SR channel interact strongly with permeating cations without hampering their rate of flux through the channel.

The principle energy barrier to a high flux imposed by a lipid bilayer membrane is the electrostatic image energy experienced by an ion in traversing a membrane. Permeation requires that the activation energy due to this energy does not make transport too slow. This is particularly expected to be a problem for divalent cations. This condition can possibly be satisfied, even for an extended (tubular) channel, by a suitable affinity profile which provides a point-for-point balance between the competing image and affinity energies; so that these are poised around the same energy level. However, it seems unlikely that the usual neutral ligands alone can provide such an energy; so that charged groups are likely to be involved. There is no difficulty imagining that a channel so constructed could be highly selective, with ions interacting intimately with the channel walls. The energy profile would insure a high conductance at the same time.

Another possible way to get both a high flux and a high selectivity would be to confine the selectivity filter to a very small and narrow region [this could be as simple as a circular array of four to six oxygen ligands occurring as a very narrow neck in an otherwise water-filled pore (*cf.* [55, 57, 80, 97, 98]). In this situation there would be no significant electrostatic image force to be overcome; and the number of jumps would be reduced to the minimum possible. Both factors would contribute to making the rate maximal for a given selectivity.

Indeed, in order to explain the discrepancy between the high conductance and low conductance K channels Latorre and Miller [80] have proposed that there are two types of biological K channels, which differ primarily in their physical lengths. The functional significance of this type of specialization is an intriguing question for future progress in understanding selectivity.

Examples of Measurements of Selectivity in Systems of Increasing Complexity

We will now discuss in detail the characterization of selectivity among species of the same charge for symmetrical one-ion channels, asymmetric one-ion channels, and for multi-ion channels.

1. The Permeability Ratio as Defined from Reversal Potentials by the Goldman-Hodgkin-Katz Equation

We first need to define selectivity as measured by reversal potentials unambiguously. When net current across cell membranes is zero, the membrane potential is the so-called reversal potential and can be described in terms of ionic concentrations and permeability ratios through the now classical Goldman-Hodgkin-Katz (GHK) equation [49, 62]

$$V_0 = \frac{RT}{F} \ln \left[\frac{(P_a/P_b)(A^+)_1 + (B^+)_1}{(P_a/P_b)(A^+)_2 + (B^+)_2} \right] \tag{2}$$

in which V_0 is the potential difference, or reversal potential, between the solutions on the two sides of the membrane; (A^+), (B^+) are the activities of the ions in the solutions; P_A, P_B are the ionic permeabilities; the subscripts 1 and 2 denote the outer and inner solutions, respectively; and R, T, and F have their usual meaning. For simplicity, we have restricted this equation to the case of permeability solely to monovalent cations.[8]

Not all, but many, membrane potential measurements have been shown to be described accurately by this equation. Examples are: ion exchanger membranes like glass electrodes [24], carriers in bilayer membranes in the equilibrium domain [39], gramicidin channels at low salt concentrations [38, 102] and the K channel isolated from sarcoplasmic reticulum [17]. The selectivity of such systems, when measured by reversal potentials, is characterized by a single parameter, the permeability ratio. This permeability ratio is not always constant under varying experimental conditions but can appear to depend on ionic composition (*see* several examples below).

We will not become involved with the obvious complications that can ensue if a macroscopically measured membrane potential contains contributions from more than one type of channel. Such a mozaic membrane situation can lead to a V-dependent permeability ratio, even in the absence of any net membrane current, owing to the presence of local circuits of current [28].

If the permeability ratios are taken as strict constants, independent of voltage and of solution concentrations, then the range of applicability of this equation is expected to be quite restricted, although a number of important situations where this equation has been shown to hold have been noted above. Of course, if the permeability ratios are taken merely as parameters, defined experimentally, which can vary arbitrarily with concen-

[8] Analogous equations valid in mixtures of permeant ions of differing valence type have been proposed [87, 99, 122] which take a variety of forms, depending on their underlying assumptions. In addition, more general forms of the GHK equation, which allow for possible effects of nonideality within the membrane, are well known both empirically [33] as well as theoretically [73]; *see also* [122] for extension of the Eisenman equation to divalent cations as well as for relevant references to the behavior of symmetrical regular solutions.

tration and voltage, then this equation can always fit any experimental set of data. We will show, in agreement with Hille [56] and Krasne [76], that in one-ion channels all apparent concentration dependences are actually due to voltage dependence of the permeability ratios.[9] In multi-ion channels true concentration dependences are encountered [6, 7, 37], which are attributable to interactions [113] and/or multiple occupancy [60, 123, 124] effects.

Symmetrical One-Ion Channels

1. Relation of Conductance Ratios to Permeability Ratios and Binding Constants

Even in the simplest situations where the GHK equation holds, the selectivity as measured by membrane conductance ratios is expected to be directly comparable to that inferred from permeability ratios only in the limit where independence holds (i.e., at low occupancy of the system where conductance is proportional to concentration). This behavior is illustrated in Fig. 10 using the data of Coronado et al. [17] for a slightly asymmetric K channel of sarcoplasmic reticulum. Note that the permeability ratio (P_K/P_{Na}) is independent of concentration, whereas the conductance ratio (G_K/G_{Na}) changes with concentration. Also note that the two ratios become the same at low concentration. The reasons for such behavior in saturable one-ion channels have been clearly discussed by Hille [56] and are related to the fact that the permeability ratio depends only upon peak energy differences (which are concentration independent for the present simple example), whereas conductance ratios also depend upon the degree of occupancy of the sites, which, of course, depends upon concentration. Figures 11 and 12 should help clarify these statements.

Figure 11 schematizes the energy profile for a symmetrical one-ion channel with a large number of equal barriers interposed between identical solutions. The relationship between the energy levels determining the hopping rate constants (mobility) and the equilibrium binding constants (which together with the aqueous ion concentration determine the occupancy) are shown on the figure. Note that these energies are defined relative to the hydrated aqueous reference energy level. The permeability ratio (P_a/P_b) between two different ion species, A and B, is defined by the products of the binding (K) and rate constants (k^*) for these species by

$$P_a/P_b = (K_a k_a^*)/(K_b k_b^*). \quad (3)$$

This permeability ratio, when inserted into the GHK equation describes the total reversal potential behavior under all possible solution conditions. In the present example the ratio is a constant, independent of concentration and voltage.

On the other hand, the conductance ratio at a given concentration, even for the present simple example, depends upon the values of conductances which can themselves be different functions of concentration for different ions, as schematized in Fig. 12, where the conductance *vs.* concentration behavior is plotted (*see* [81] for more details). The binding constant determines the half-saturation point on the curve (the reciprocal of the binding constant is given by the concentration at which the conductance has half its maximal value); while

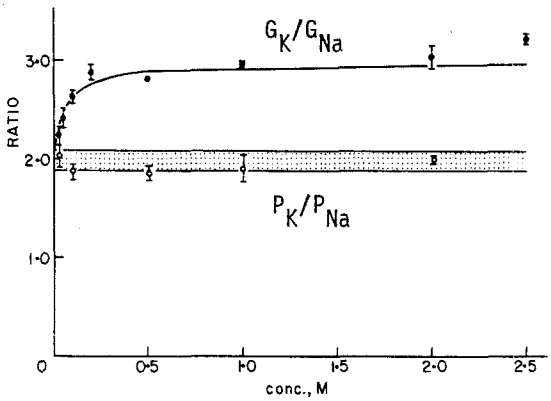

Fig. 10. Concentration dependence of channel selectivity (after Fig. 6 of [17] with slightly revised labeling). The conductance ratios measured under symmetrical conditions are plotted as filled circles with the continuous curve representing the expectations for a one-ion model; while the permeability ratio measured under bi-ionic conditions are plotted as the open circles and stippled region. (Described in text)

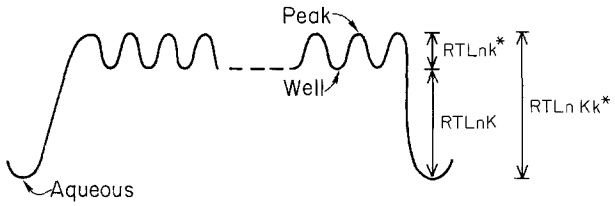

Fig. 11. Schematic profile for a symmetrical one-ion channel with a large number of equal barriers separating identical solutions. (Described in text)

[9] Thus, in such channels if one could arrange all concentrations so that the reversal potential were constant, then a constant permeability ratio would be observed. Conversely, even in one-ion channels if the experimental conditions give differing reversal potentials, different permeability ratios will be observed except if one is dealing with a symmetrical one-barrier system or if, in a multi-barrier system, Hille's constant peak energy offset condition is fulfilled. These conclusions follow from Hille's [57] Eq. (3).

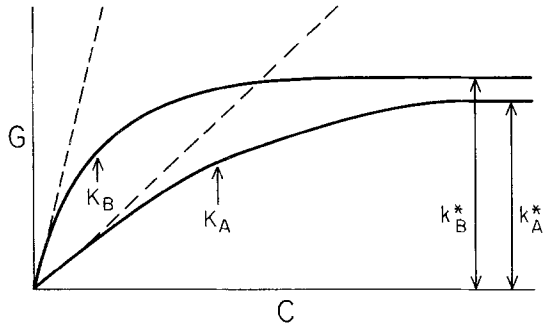

Fig. 12. Diagram illustrating the interrelations between permeability, conductance, and binding defined in Eq. (3) and showing why the ratio of conductances for two different ions, *A* and *B*, can depend upon concentration even in the simplest one-ion channel. (Described in the text.) The rate constants, k^*, correspond to the maximum rate in the limit of high concentration. The location of the binding constants, *K*, are indicated at the concentrations at which the conductances have half their maximum values. These concentrations correspond to the dissociation constants, which are the reciprocals of the binding constants

the hopping rate constant determines the maximum limiting conductance, seen at high concentrations. Indeed, the conductance at any particular concentration is given in terms of both of these constants by a Michaelis-Menten type of equation, which therefore defines the conductance ratio between two ions explicitly.

In the limit of low ion concentration (dashed lines) the ratio of conductances does indeed equal the permeability ratio. However, at all concentrations showing a departure from these lines it is clear that the conductance ratio will generally differ from this low concentration limiting ratio, becoming simply the mobility ratio in the high concentration limit. This is, of course, the situation which prevails in a macroscopic ion exchanger membrane like glass, whose sites are always occupied by virtue of the electroneutrality constraint.

It should therefore be apparent from the above that the permeability ratio, as defined from reversal potentials using the GHK equation, is a simpler measure of selectivity in a one-ion channel than the conductance ratio, which generally cannot be used to specify selectivity uniquely without providing additional information as to the degree of saturation of the channel under the experimental conditions and the maximum limiting conductances for the various species. The conductances themselves, however, are important in that, together with the $I-V$ shape, they provide necessary information for defining the energy profile of the channel and thus enable one to extend selectivity considerations to the more fundamental level of comparison of energy profiles.

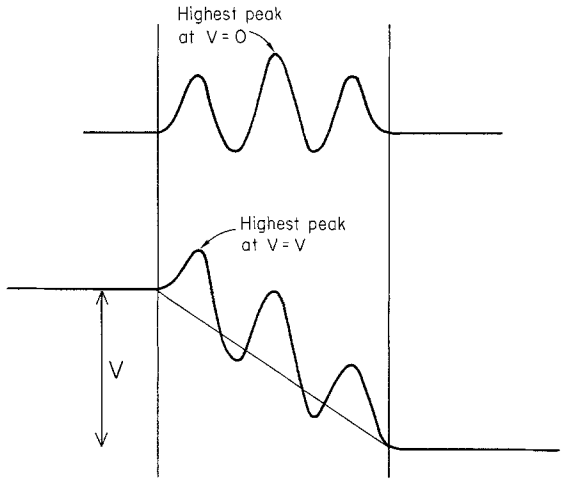

Fig. 13. Diagram of the effect of applied transmembrane potential on the electrochemical potential energy profile. (Described in text)

2. Voltage-Dependent Permeability Ratios

The simplest situation in which a voltage-dependence of the permeability ratio occurs is when there are several different rate-determining barriers at different locations in the potential field. How this happens can be made intuitively clear by Figs. 13 and 14; but the reader is referred to Hille [57] and Krasne [76] for more details, as well as to the further discussion of this in Figs. 19–20 using the gramicidin channel as an example.

Figure 13 shows the effect of an applied transmembrane potential on the electrochemical potential energy profile for a channel whose profile at zero transmembrane potential is given above. Notice that whereas in the absence of an applied potential (in the upper portion of the figure) the central peak is the highest (and therefore the most important one in determining the rate), the peak at the membrane interface becomes rate determining (e.g., higher) when a potential is applied in the lower portion of the figure. This is an example of the location of the rate-determining step shifting with potential because of the different potential dependences of barriers located at different places in a potential field (in this example, the central barrier has a strong voltage dependence because it "sees" half the applied potential; whereas the barrier at the membrane surface has little potential dependence).

An experimental example of the above effect is given in Fig. 14 for a typical experimental system, the cation carrier trinactin in a glyceryl dioleate bilayer (voltage-dependent permeability ratios occur for the same reasons for carriers as for channels). In this symmetrical 3-barrier system the profile is like that of Fig. 13; but which barrier

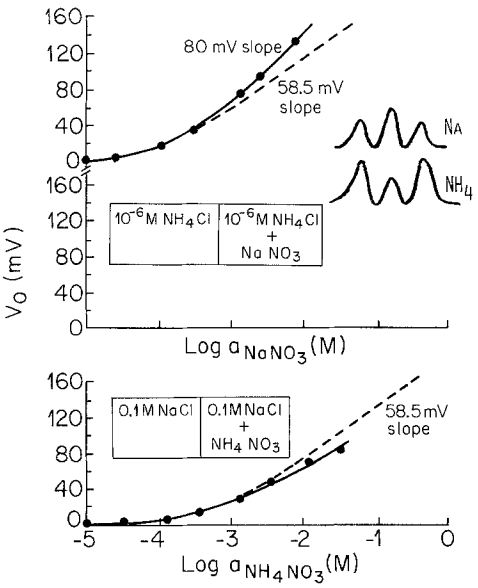

Fig. 14. Illustration of apparent concentration dependence of permeability ratio due to different locations in the potential field of the rate-determining barriers for different species. For the example of trinactin [34] shown here, the principal barrier for NH_4 is at the membrane surface while that for Na is in the middle of the membrane, as indicated in the energy diagrams. If the permeability ratio were constant, the data points would fall on the dashed curves drawn with Nernst slope of 58.5 mV per decade. The observed data points for Na added to one side of a membrane separating 1 μM NH_4Cl (upper diagram) can be seen to deviate from this expectation, falling on a curve whose slope is 80 mV. On the other hand, the observed data points when NH_4 is added to one side of a membrane separating 0.1 M NaCl solutions (lower diagram) fall below the dashed Nernst curve on one whose limiting slope is considerably less than 58.5 mV per decade. In both cases, the data would be interpreted as showing a nonconstant permeability ratio; but the actual cause is due to an explicit voltage dependence [14] which produces the theoretically expected continuous curves as a consequence of the changes of reversal potential with concentration, as described in the text

is the largest depends upon the ionic species. For Na the middle barrier (to translocation) is the largest; whereas for NH_4 the outer barrier (to unloading) is the largest [31], as indicated by the energy diagram on Fig. 14. The different voltage dependences of these barriers do indeed produce quite complicated changes in the apparent permeability ratio as measured by reversal potentials in the ionic mixtures indicated by the diagrams in Fig. 14. This is shown by the deviation of the data points in the figure from the dashed curves which would be expected from the GHK equation for a constant permeability ratio. The points in the upper figure plot the experimentally observed reversal potential when Na is added to one side of a membrane initially separating identical solutions of 1.0 μM NH_4Cl. The GHK equation predicts a Nernstian 58.5 mV slope at high Na activity, and the data points can be seen to deviate seriously from this expectation, showing supra-Nernstian slope of over 80 mV. In the lower figure, the experimental data points are for the converse experimental situation where NH_4 is added to one side of a membrane initially separating identical solutions of NaCl (0.1 M). Here the experimentally observed reversal potentials deviate in the opposite direction from the GHK expectations, being sub-Nernstian.

If one calculated apparent permeability ratios for each data point using Eq. (2), one would have to conclude that the permeability ratio between Na and NH_4 appeared to vary with concentration. But the concentration dependence in the present example is indirect because the permeability ratio is actually a function of voltage alone. This is illustrated by the solid curves which have been drawn according to the theoretical expectations [14] for a carrier-mediated permeation with an energy profile like that in Fig. 13. In this situation the reversal potentials obey the GHK equation with concentration-independent permeability ratios provided that their voltage dependence is explicitly stated (for the explicit voltage dependence *see* [31], Fig. 2). The apparent concentration dependence therefore occurs because changes in concentration change the reversal potential and as a consequence, since the relevant peaks lie at different locations in the potential field, changes in concentration change the relative importance of the different peaks.

Asymmetric One-Ion Channels

1. Definition of Symmetrical and Asymmetric Channels

At this point we need to define more carefully the meaning of a symmetrical channel. This is a channel in which an ion experiences the same energy profile, when traveling one way across a channel, that it experiences when moving in the opposite direction. For example, it has been proposed that the selectivity filter of the acetylcholine receptor channel is located near the intracellular membrane surface [65, 66, 68, 92]. Cations entering this channel seem to encounter larger energy barriers near the intracellular, than the extracellular, membrane surface. This is an *asymmetric channel.* By comparison the gramicidin channel, composed of two identical monomers in each monolayer of a lipid membrane, is a *symmetrical channel.* Note that although the channel is symmetrical, an individual barrier may have an asymmetric shape in that the voltage dependence for hopping across it may depend on the direction of its movement.

Voltage-dependent permeability ratios can be especially misleading in the case of asymmetric channels. As we will demonstrate, concentration-dependent permeability ratios, which are a consequence of a voltage-dependent shift from one barrier to another, can be observed in such one-ion channels, which could erroneously be used as evidence for multi-occupancy. We consider this an important topic to explore, since the energy profile experienced by an ion in biological channels is usually asymmetric with respect to the plane of the membrane [6, 7, 17, 57, 65–68, 97]. This has considerable consequences for the theory of ion permeation and selectivity, which has been primarily based, to date, on the assumption that ionic channels are inherently symmetrical. Since the effects of asymmetry in channels is a little-explored area (but *see* [57]), we felt it would be worthwhile to carry out systematic simulations on a simple model for an asymmetric channel.

Simulations on a Model Asymmetric One-Ion Channel

The purpose of this section is two-fold. First, we will show when the permeability ratio, as defined by the GHK equation, is dependent on ion concentration and when it is not, for a variety of energy profiles. Second, we will consider the usefulness of the permeability ratio for diagnosing the type of channel (one-ion, multiple-ion, asymmetric, etc.). Many of the rules about the concentration dependency of the permeability ratio, which hold for symmetrical channels, will be shown to be immediately violated in the asymmetric situation.

1. Measurements of Selectivity

One classical tool for assessing selectivity is the permeability ratio, P_a/P_b, as defined from the reversal potential according to the GHK equation. There are four experimental protocols usually used to obtain P_a/P_b as a function of ion concentration of the two species, a and b. They are listed below.

I. *Biionic*

In the biionic case one side of the membrane contains one species, and the other contains the other species, in equal concentrations. In examining concentration dependences in a biionic experiment the concentrations of each side are changed in equal amounts.

II. *Constant Ratio*

This case is similar to the bionic case, in that one species is on one side of the membrane, and the other species is on the other side. However, the ion concentrations are not equal, but maintained in some fixed ratio to one another. For example, one side may be twice as concentrated as the other. If the concentrations of each side are increased by a factor of ten, the experiment is a constant ratio experiment.

III. *Mole Fraction*

In this case one side of the membrane is held fixed at a given ion concentration. The other side contains a mixture of the two ions at the same total concentration. The proportions of the mixture can be varied while holding the total concentration on that side constant.

IV. *One-sided Addition*

In this case the reversal potential is measured while increasing the concentration of one ion only on one side of the membrane. The initial concentrations of the two ions on each side of the membrane are arbitrary.

2. Simulations of a Simple Two-Barrier Model

We have examined a variety of simple asymmetric channels, in order to assess the usefulness of P_a/P_b as a tool for providing information about an unknown channel. We have used a one-site, two-barrier Eyring model for simplicity (Fig. 15), but anticipate that other types of models with more barriers or wells will yield similar results. For simplicity we assume that the site exists in the middle of the electric field, and the barriers may be located at arbitrary locations and have arbitrary energy levels with respect to free solution. We have also allowed the possibility that barrier locations may be specific to the ion species. Many types of asymmetric barrier arrangement are possible in this simple model (Fig. 15), and the measurement of P_a/P_b using the above experimental protocols can provide some information about the type of asymmetry. The results of simulations of such experiments are shown in the Table 1.[10]

[10] The method for calculation of the current (or flux) through a simple two-barrier, one-site model has been given previously [56, 81]. We have added only two complications. First, Hille's constant offset peak constraint is not imposed, and second, the barriers may have an asymmetric shape [64, 92]. We used this model to calculate net ion flux through the channel as a function of membrane potential and ion concentration. Then we used Brown's algorithm in a Levenberg-Marquardt procedure [11] to minimize the square of the flux with respect to membrane potential. The resultant membrane potential was the reversal potential, which was then inserted into the GHK equation to give the permeability ratio.

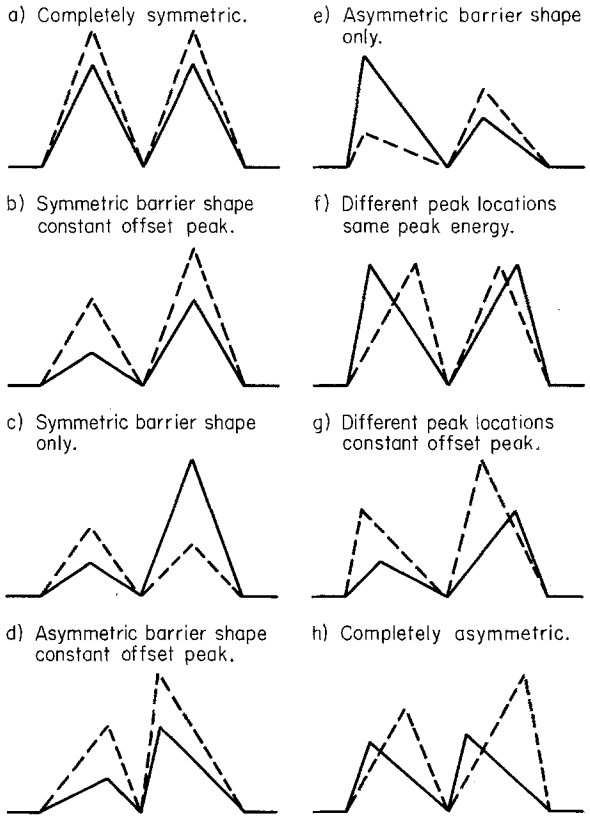

Fig. 15. Various energy profiles for a one-site, two-barrier channel. The solid and dashed lines represent profiles for two different ions. (Described in text)

Table 1.

Barrier profiles (*see* Fig. 9)	Experimental protocols			
	I Biionic	II Constant ratio	III Mole fraction	IV One-sided addition
a)	–	–	–	–
b)	–	–	–	–
c)	–	–	*	*
d)	–	–	–	–
e)	–	–	*	*
f)	–	–	–	*
g)	–	–	*	*
h)	–	–	*	*

– indicates concentration-independent permeability ratio.
* indicates concentration-dependent permeability ratio.

If P_a/P_b is dependent on concentration, then we say, arbitrarily, that a violation occurs for the specific experimental protocol. The use of the term "violation" refers to the fact that concentration-dependent permeability ratios traditionally have been [6, 37, 38, 123] interpreted to mean that a channel can be occupied by more than one ion at a time. Note that, although the permeability ratio may be concentration-independent for several different protocols, it is not necessarily the same for each protocol. However, if it is concentration-independent for all protocols, then it must be the same for each one.

The results of Table 1 can be summarized as follows. P_a/P_b is completely independent of concentration only for symmetrical models (*a*) or simple asymmetric models which obey the constant offset peak condition (*b*, *d*), in accordance with Hille [56]. The reason for this is that the only way the permeability ratio can change in a one-ion channel is by a shift in the relevant peak heights due to a change in voltage. If a channel obeys the constant offset peak energy condition (even if it is asymmetric), then concentration-dependent changes in reversal potential only cause a shift from one rate-limiting barrier to another, each with the same selectivity.

For asymmetrical models, as soon as the constant peak offset condition is abolished, violations occur for protocols III and IV, although there are no violations in protocols I and II. This is because the latter protocols do not produce concentration dependent changes in reversal potential.

In the class of models where barriers are not located in the same location for each ion species (*f*, *g*, *h*), further refinement is possible. If all barriers have the same level, but arbitrary locations in the field (*f*), then a violation occurs only for protocol IV. All further complications (*g*,*h*) lead to violations in both III and IV, but not in I or II, for the same reason.

We have not found any barrier arrangement which produces violations of bi-ionic or constant ratio experiments, protocols I and II. This is because there are no shifts in voltage between the two barriers when the concentration is varied in such experiments and, consequently, no changes in observed permeability ratios even when both barriers are contributing to the overall ratio observed.

The implications of this latter finding are immediately apparent. If one wishes to argue from the observation of a concentration-dependent permeability ratio that a channel can contain more than one ion at a time, it is necessary to observe this using either protocol I or II. Frequently in experiments on biological membranes, protocols III or IV are more convenient, or even necessary. Our analysis suggests that these types of experiments must be interpreted with caution.

The above observations lead to certain useful generalizations. For example, when dealing with

reversal potential selectivity in a one-ion channel, it is possible to attribute any apparent variation in permeability ratio to a change in the difference in peak energy heights, always referred to the aqueous solutions. Recall that from the usual form of the potential in the GHK equation, which contains only concentrations and permeabilities, such a variation must show up as an apparent concentration dependence of the permeability ratio.

In a one-ion channel, however, such an apparent concentration dependence can be shown [57, 76] actually to be due to a voltage dependence of the permeability ratio which occurs, for example, if the change in concentration alters the barrier heights (in a channel with more than one barrier) differently for each of the ions whose permeability ratio is being measured. For example, if two barriers are significantly involved in the permeation of each ion and the left-hand barrier is larger for species A and the right-hand barrier is larger for species B, a concentration change that produces a change in voltage will alter, through the voltage effect on the two peaks, the relative importance of each barrier for each species and hence alter the permeability ratio. Conversely, if the experimental conditions can be arranged so that the reversal potential is constant, the permeability ratio will be observed to be constant.

In accordance with previous analyses for channels containing no more than one ion at a time [56, 81], P_a/P_b is independent of the energy level of the well for either ion species. This can be shown to hold rigorously for all types of asymmetry in one-ion channels with more barriers and wells than in the above example (Horn and Eisenman, *unpublished calculations*). This fact holds even though the relative occupancy of the well by each species can change drastically. However, this is no longer true in multi-ion channels (*see* later section).

All these findings are consistent with the intuitive extension of the conclusion already reached for one-ion channels more generally [56, 57] that only the peak energies are pertinent to the permeability ratio. Thus, when the permeability selectivity of a channel is made up of the combined contributions due to several peaks, concentration changes *per se* do not change the observed permeability ratio through the occupancy of the wells, but only by changing the voltage at each peak so that its contribution to the overall permeability ratio is altered. Direct effects of concentration to shift the levels of the peaks themselves are only possible in a multi-ion channel.

One obvious procedure for assessing whether or not a one-ion channel is symmetrical, is to measure a reversal potential under two bionic conditions: first when species A is on the left and species B is on the right side of the membrane, and then when their relative locations are inverted. Only a symmetric channel will have the same reversal potential in each case.

3. Anomalous Sequences Produced by Asymmetric Channels

If the barriers in a one-ion-channel are merely asymmetrically located, but have identical selectivity (Fig. 16*A*), both in sequence and in magnitude, we find by an extension of the above type of analysis that the selectivity of the channel itself, measured by P_a/P_b, is the same as that of the individual barriers. This is equivalent to Hille's [56] constant offset peak condition. However, for an asymmetric biological channel, it is unlikely that all barriers will have identical selectivities. For example, if a channel has two prominent barriers, one of which is the selectivity filter and the other relatively nonselective (Fig. 16*B*), then what can we predict about the selectivity of the channel as a whole? We examined this question by using a simple version of the above model in which the barriers are symmetrically located 1/4 of the way through the field from the edge of the membrane, and the well is located in the middle of the field and has the same energy level as free solution for each ion species. We have examined two cases. In the first (Fig. 17) the selectivity of one barrier is Eisenman sequence I and the other is sequence XI, with the relative magnitudes determined according to a simple coulombic model (*see* [23]).[11] In the second case one barrier is nonselective, while the other barrier has any given selectivity sequence (for example, *see* Fig. 16*B*).

It is probably instructive to examine the first case in some detail. The barrier structure is drawn to scale in Fig. 17. Barrier 1 on the left has a sequence I selectivity, being most permeable (relative to water) to Cs, and barrier 2 has a sequence XI selectivity. We used the GHK equation to determine the permeability ratio with respect to Cs, which was always the only cation on the left side of the membrane. The test cation was the only cation on the opposite side of the membrane.

Using this model we obtained the following re-

[11] We should point out that this assignment of selectivity pattern is completely arbitrary. Even if the barrier represents the interaction between the cation and a simple ligand, like a carbonyl oxygen, the energetics of the interaction are likely to be much more complicated than that expected for a simple coulombic model, because of the unknown interactions with water molecules.

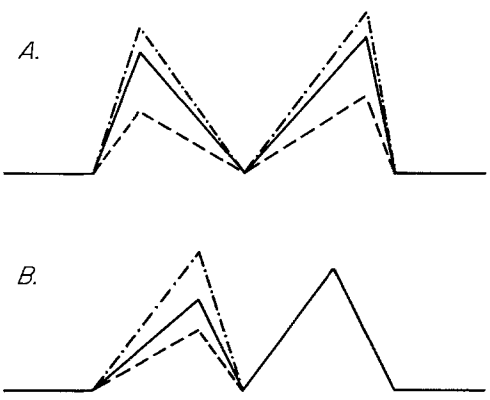

Fig. 16. Energy profiles for a two-barrier channel. (*A*): Asymmetric barrier profiles for three different species. Each barrier has same selectivity. (*B*): One barrier is nonselective

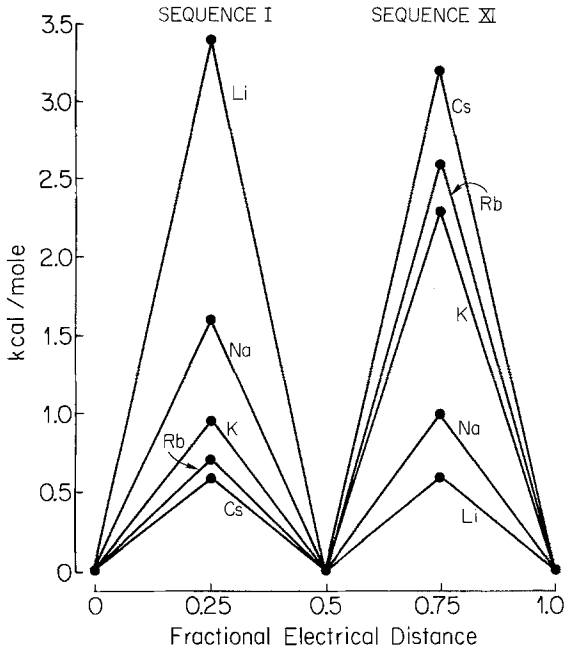

Fig. 17. Two-barrier channel. Left barrier has a sequence I selectivity. Right barrier has sequence XI selectivity

sults. Using Protocol I when the concentrations of Cs and the test cation were equal, the selectivity sequence obtained was Li > Cs > Rb > K > Na. This is a polarizability sequence, which is immediately obvious from plotting the logarithm of the permeability ratio against inverse ionic radius in Fig. 18 (case [Cs] = [M]). The concave upward shape, as discussed in a preceding section, is the topological trademark for this type of pattern.

We further examined this example using Protocol II by making a concentration gradient across the membrane. When Cs was 10 times more concentrated than the test cation (case [Cs] = 10[M]), the permeability sequence was Cs > Li > Rb > K > Na. However, when Cs was 10 times less concentrated than the test cation (case [Cs] = 0.1[M]), the sequence was Li > Cs > Rb > Na > K. Interestingly, these examples are also polarizability sequences, as shown in Fig. 18. Concentration gradients thus cause a change in the selectivity sequence, essentially producing variations on the same general pattern.

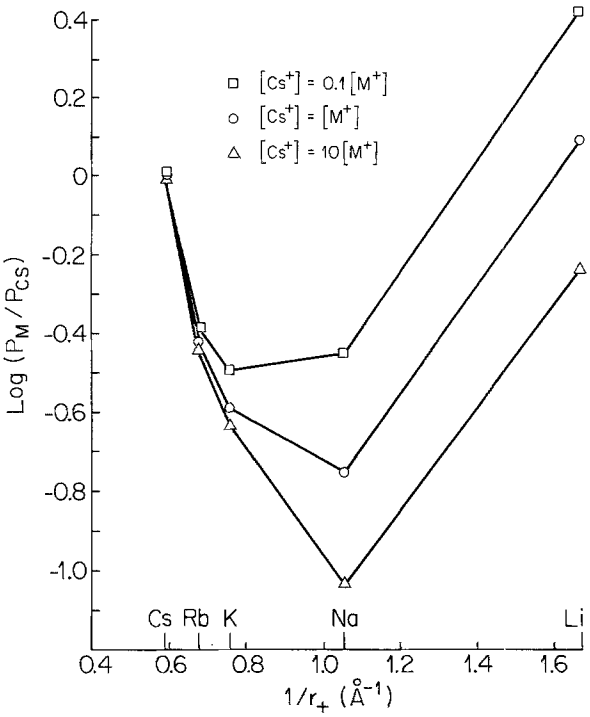

Fig. 18. Selectivity of channel shown in Fig. 17 from reversal potentials. Selectivity is given for three different relative concentrations between Cs and a test cation

Qualitatively, these effects can be understood as a shift in the importance of one or the other barrier. When Cs is more concentrated than the test cation, barrier 1 is more rate limiting due to the increase in electrochemical potential on the left side of the membrane. Since barrier 1 has a high selectivity for Cs, the observed finding of a higher channel selectivity for Cs is to be expected. On the other hand, when the Cs is less concentrated on the left side of the membrane, one expects the sequence XI barrier to be more rate determining. In accordance with this expectation the observed sequence in this situation favors the Li-selective barrier, as seen in Fig. 18.[12]

The above simulation shows that a simple arrangement of two coulombic barriers can yield a

[12] It can be shown rather easily that if the concentration gradient is sufficiently steep, only one of the two barriers is rate limiting. In that case the selectivity sequence of the channel is the same as that of the rate-limiting barrier. This may be a useful experimental tool to examine barriers preferentially on either side of the membrane.

pattern of permeability sequences which superficially interpreted would seem to indicate a polarizability pattern (this bears on the interpretation given by Reuter and Stevens [109] to their non-Eisenman sequence, which shows an anomaly of the polarizability type in that Li is anomalously highly permeable (*recall* Fig. 8)).

Finally, when we examined the effect of making one barrier nonselective (Fig. 16*B*), the selectivity sequence of the whole channel was found to be the same as that of the other barrier. However, the *magnitude* of selectivity was decreased by the nonselective barrier. The resulting selectivity was not, in general, a simple scaling of the original pattern, but more complicated, and depended on the relative amplitudes of the two barriers.

In conclusion our analysis shows that the interpretation of the magnitude and sequence of selectivity of asymmetric multi-barrier channels may be extremely difficult, even in the simplest cases. Irregular patterns may be produced by a series of very simple barriers, each of which is in all ways regular. Clearly, to avoid confusion it will no longer suffice to compare overall selectivities by such antique measures as the permeability ratio; rather, it will be necessary to compare the energy profile underlying selectivity, barrier by barrier and well by well.

Multi-Ion Channels

Multi-occupancy is well-established to exist in channels and has been detected by one or more of the following criteria. (i) The flux ratio exponent is greater than unity [4, 63]. (ii) The concentration dependence of single-channel conductance exhibits a maximum [37, 123]. (iii) permeability ratios measured from reversal potentials are concentration dependent [6, 37]. And (iv) blocking ions show unusually high voltage dependencies [58]. By these criteria a number of important channels, exemplified by Na and K channels [4, 6, 58, 63] and the gramicidin channel [37, 38, 106, 114, 123] have been found to be occupiable by more than one ion. As far as selectivity is concerned, we will discuss only cirterion (iii) in detail.

Selectivity in channels occupiable by more than one ion follows the same energetic principles as above but can be more complicated. In particular, it appears from the work of Hille and Schwarz (*see* Fig. 11 of [58]) and of Kohler and Heckmann [74] that peak energy differences no longer suffice to define the permeability ratio. Only in the particular case of a channel with only one significantly rate determining barrier is the permeability ratio still defined by the peak energy difference (*cf.* [113]). Thus, a description of selectivity, even if limited to that seen in the simplest phenomenon, the reversal potential, generally will require a detailed knowledge of the complete energy profile (including the energy wells) for every occupancy state. Because this field is in its infancy, we will confine ourselves here to symmetrical channels and point out only the most salient features of these together with examining the properties of the gramicidin channel to illustrate concretely certain key points.

1. Channels with Only One Rate Determining Barrier

Peak energy differences still suffice to define the permeability ratio in multi-ion channels provided they contain only one significantly rate determining barrier. This has been examined for a symmetrical channel by Sandblom et al. [113] and used by Eisenman et al. [38] for an initial interpretation of reversal potential data for the gramicidin channel. Unfortunately, the current-voltage behaviors for all presently known multi-ion channels indicate that it is unlikely that any of these can be represented by a model with only one significantly rate determining barrier; so this simple case is not likely to prove useful.

2. Channels with More Than One Rate Determining Barrier

In channels with more than one rate determining barrier a number of complications can appear. First, it appears that, except in the low occupancy limit, where the channel is usually unoccupied due to low ion concentration, the permeability ratio is no longer solely determined by the peak energy differences in a multi-barrier, multi-ion pore; for Kohler and Heckmann [74] have shown that at high occupancies the permeability ratio also depends on the binding affinities of the sites. This is in accord with the prior demonstration by Hille and Schwarz [58] that anything (e.g., binding) which changes the relative probabilities of different occupancy states can affect the permeability ratio and the conclusion of these authors that the energy wells, which determine ion binding, can make a contribution to the permeability ratio which is distinct from that made by the peaks.

Second, even in the low occupancy limit where peak energy differences alone determine the permeability ratio, two kinds of complications can be anticipated: (*A*) It may be that in a channel with several barriers, the one that is rate determining

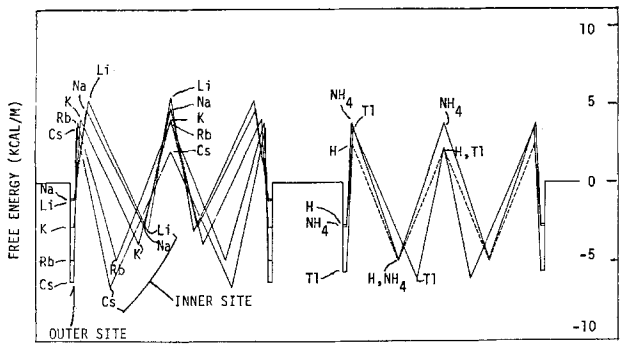

Fig. 19. Free energy profiles for the indicated cations in the one-ion loading state of the gramicidin channel [35] to illustrate how various complications in the interpretation of reversal potential selectivity can occur due to different locations of the major peaks. (Described in text)

for one ion species is different than the one that is rate determining for the other ion species, a situation that will be shown below to occur in the gramicidin channel. (*B*) Even if the same energy barrier is rate determining for the two species, this barrier may not lie at exactly the same location in the potential field, a situation also found in the gramicidin channel.

3. The Gramicidin Channel as an Example

Because it is the best characterized of all multi-barrier, multi-occupancy channels, both as to structure and as to behavior, we devote some space here to the selectivity of the gramicidin channel.[13] This will enable us to provide some concrete examples of the kinds of behavior that can be anticipated in its biological counterparts, which have the additional complexity of being likely to be asymmetrical as well. We begin with the energy profile for various ions and for various occupancy states and then discuss some implications of this for selectivity more generally.

The Energy Profile at Low Occupancy

Figure 19 plots the energy profile (in the potential field) for the gramicidin channel in its lowest (one-ion) occupancy state and clearly illustrates a number of features that of particular pertinence to selectivity. The group Ia cations are shown at the left; while Ti, H and NH_4 are shown at the right. The energy profiles in this figure and in Fig. 20 come from a recent analysis [35] of extensive electrical (as well as flux) data according to a three-barrier four-site model [112].[14] In traversing this model for such a channel each ion encounters successively: an outer site, an entrance barrier, an inner site, and a central barrier; followed by the corresponding sites and barriers on the other side of the channel. The following characteristics are immediately apparent from this figure. First, although all barriers and wells lie in roughly the same locations for all ionic species, on close scrutiny clear species differences are apparent in the precise positions of these in the potential field. We begin with the group Ia cations.

Group Ia Cations

Consider first the *locations* of the energy peaks and wells. The top of the entrance barrier is almost at the mouth of the channel in the case of the larger ions, whereas for the smaller ions it lies considerably further in (for Cs there is virtually no voltage dependence of the entry step (1.4%), whereas for Li there is a significant voltage dependence of this step (7.4%)). The outermost well is assumed to lie at the same place for all species (external to any significant potential drop), but the inner well is found to be much further into the channel in the case of the smaller ions than in the case of the larger ones (for Cs the internal site senses 18% of the applied field; whereas for Li it senses 38%). This has the consequence that the voltage dependence for leaving the channel is much larger for the smaller ions (31% for Li) than for the larger ones (17% for Cs).

Comparing next the *heights* of the entry barrier (i.e., the differences between outer wells and peaks), it is seen that the smaller ions encounter a much smaller barrier in entering the channel from the outer site than do the larger ions (the entrance rate constant is 1.9×10^{-8} sec^{-1} for Li in contrast to 4.6×10^{5} sec^{-1} for Cs [35]). Similar, but less pronounced, differences are seen in the barriers for leaving the channel as well as for crossing it. Thus, the larger ions have more difficulty entering, crossing, and leaving the channel than do the smaller ions.

[13] Although the permeation of gramicidin has received considerable attention (*cf.* [41, 83] for recent reviews), less attention has been given to its selectivity. Indeed, this channel is still generally regarded (*cf.* [80]) as resembling an aqueous pore, much as was concluded from the original characterization [59, 102]. This is partly because of the apparent correlation between aqueous mobilities and channel conductances (at high concentrations) found initially [59]. However, it is becoming increasingly apparent that the selectivity of binding is considerable [18, 38, 125]. Some consequences of this will be examined here.

[14] Whether or not this particular model, which at the very least describes the experimental data satisfactorily, proves ultimately to be correct, it can be used as an instructive example for the purpose of illustrating a number of complexities that are likely to be encountered in analyzing the selectivity of any multi-barrier channel.

Despite this, it can be seen from examining the levels of the peaks in Fig. 19 that the permeability to larger ions is greater than that to smaller ions. (i.e., the peak energies for the larger ions are less elevated above their aqueous levels). This is because the strong affinity of the larger ions for the outer binding site lowers the energies of the adjacent peaks (relative to the aqueous reference solution) more than the difficulty of leaving the site raises them. Such behavior shows how a strong affinity can lead to a high permeability.

Also note that there is substantial binding selectivity apparent from the large differences in the depth of the *wells* in Fig. 19. For example, the affinity of the outer site differs by a factor of 7,000 between Cs and Li while that for the inner site differs by a factor of 400 (the outer site binding constants for Cs and Li are 700 *vs.* 0.1 M^{-1}, whereas those for the inner sites are 1,200 *vs.* 3.18 M^{-1} ([35], Table 1)). This finding is of interest in view of what initially appeared to be a low selectivity for the overall permeation process in the gramicidin channel [59, 102]. Opposing effects of wells and barriers, together with energy shifts with increasing occupancy has obscured the realization of this for some time; so that the gramicidin channel is far from being the relatively uninteresting (from the viewpoint of selectivity) aqueous pore it was once thought to be. The same may be true for the end plate channel where a similar situation appears to prevail since Hille's group [2] finds substantial binding selectivities despite the low overall permeability selectivities.

A Comment on Binding Selectivity and Permeation

A clear example of how binding enhances permeation comes from the comparison of Li and Cs energy profiles in Fig. 20. From the smaller barrier heights to Li than to Cs, Li clearly moves more easily in the channel. Despite this, Cs is found to be the more permeable ion by far. The cause of this is the strong binding affinity for Cs, indicated by the much deeper energy wells for Cs than for Li. This is a good example of how binding enhances permeability by lowering the peak energies. One consequence of a high binding affinity is that it can enhance the permeability to species present at such low concentrations that they are usually disregarded. H is normally such a species at physiological pH; and the H permeability recently demonstrated to exist in biological channels [121] might be a simple consequence of the presence of a high affinity site.

Examples of Possible Complications in the Interpretation of Reversal Potential Selectivity Due to Species Differences in the Locations of the Major Peaks

How complication *B*, noted in the preceding section 2, can arise should now be apparent; for it can be expected from Fig. 19 that there should be an apparent concentration dependence of the permeability ratio (due actually to a voltage dependence) between any two species whose peaks lie at significantly different positions (e.g., Cs *vs.* Li in Fig. 20) in the potential field.

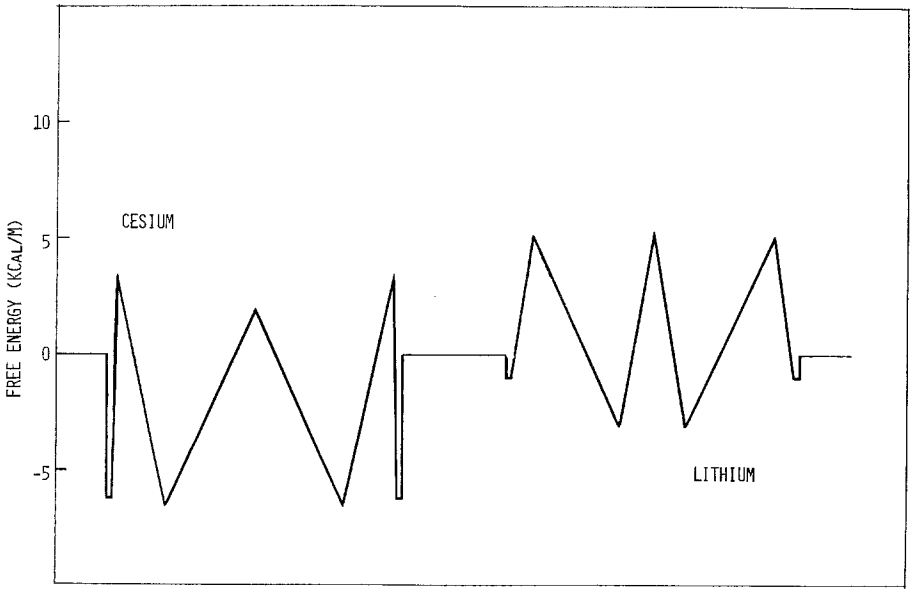

Fig. 20. Comparison of energy profiles for Li *vs.* Cs in the gramicidin channel. (Described in text)

How complication *A* can arise is seen most easily in Fig. 20, which compares the energy profiles for Li and Cs in the one-ion occupancy state. Here the highest peak for Cs is seen to be at the mouth of the channel, whereas for Li the highest peak is in the middle of the membrane. So, if one compares Li *vs.* Cs selectivity from permeability ratios measured from reversal potentials even in the limit of low ion concentration where the permeability ratios are determined solely by peak energy differences, one is really comparing the effects of the outer peak for Cs with the inner peak for Li, which can lead to confusion. The meaningful comparison here is clearly not going to be the overall permeability ratio but the comparison between the relative heights of the corresponding peaks for these ions.[15]

H, NH_4, and Tl

The profiles for H (actually H_3O), NH_4 and Tl are shown to demonstrate that these species do not differ qualitatively from the other monovalent cations since they encounter the same kind of energy profile. Their quantitative behavior is of interest for the information that it can provide as to ligand type and orientation, as mentioned in an earlier section. In particular, the profiles for H and NH_4 show that their sites and barriers are located at the same places. However, the barriers for entering, leaving and crossing are all smaller by about 1.4 kCal/M for H than for NH_4, consistent with the rate constants being about 10 times faster for H than for NH_4. Such a result would be expected if the binding of H and NH_4 both involved significant H-bonding to channel ligands, but with an additional Grotthus jump process being available for the proton in the case of H_3O. (An interesting consequence of this is that H should be able to slip past any water plug so that its diffusion rate is not limited by that for water.) The similarities between H and NH_4 strongly suggest that any channels known to be permeable to NH_4, such as biological acetylcholine-activated, Na and K channels, should also be permeable to H.

The energy profile for Tl, and its corresponding binding and rate constants is also reasonable for a polarizable species of its size, being located at a position intermediate between Rb and K. The values of binding and rate constants indicate, however, that Tl is supra-Ia (as defined in [30] with regard to its binding in all occupancy states. It is also supra-Ia with regard to its permeability as judged by the peak heights in Fig. 19.

[15] This example, since it is based upon channel properties measured in single salts and not in ionic mixtures, applies to reversal potentials strictly only under conditions of independence or constant peak offset energies; but this restriction alters none of the conclusions drawn here.

4. Conclusions

It thus appears that for multi-barrier channels the classical electrical measures of selectivity, namely the permeability ratios and conductance ratios, are beginning to lose their crispness. It seems that time has come to supercede these concepts with more fundamental ones, which we suggest can only come from a detailed characterization of the energy profile for ion permeation. A classical Rate Theory approximation may suffice or it may be necessary to use more dynamic approaches to the underlying energetics, which can then be related to any selectivity theory which is itself couched in energetic terms.

In particular, the *descriptive* questions as to selectivity now become such ones as: How many barriers are there? How many wells? Where are they in the potential field? What is the selectivity of each well and barrier? To answer these questions it now becomes desirable to carry out current-voltage studies for each ion over a sufficiently wide concentration range to characterize the I–V behavior for the empty channel, as well as for the highest occupancy state experimentally accessable; for such measurements give information on the levels and locations of the energy wells and the barriers (*cf.* [35]). Measurements of the flux ratio exponent, on the other hand, provide independent, and sometimes crucial, information about the *peaks* alone [41, 112]. Since measurements of selectivity by reversal potentials require the simultaneous presence of more than one permeant species, it may, moreover, be necessary to extend the *I–V* studies to ionic mixtures.

The *theoretical* questions become: Is Rate Theory really rigorously applicable? Or is it merely a useful formalism? Are the inferred barriers and wells simple or compound? And where are they physically located, as opposed to their formal location in the potential field? Finally, what are the implications at the molecular level of the observed selectivity?

Emerging Problems in the Dynamic Aspects of Permeation

1. Gating

So far our discussion of selectivity has been restricted to the properties of the channel when it is open, as separate from any consideration of selectivity in its gating. There are some indications

that the gating of biological channels can exhibit ionic selectivity (e.g., acetylcholine receptor channels: [46]; potassium channel: [119]; and the lifetimes of gramicidin channels appear to be related to their occupancy in a species-dependent manner [95, 110]). It is conceivable that such selectivity could merely reflect the selectivity of binding, and thus of occupancy (*cf.* [92, 110]), but it is likely to be more complex [2, 120]. This subject is in too early a stage to be included in this topical review; and we therefore will say no more about it.

2. A More Dynamic View of the Open Channel

Our conclusions concerning selectivity of the open channel so far have contained implicitly a particular set of constraints about channel structure and the energy profile for permeation. Implicitly we have been assuming that the energy profile is a constant for a given occupancy state, which, as Lauger and his colleagues [44, 84, 85] have pointed out, occurs really only in two limiting situations: namely, when the channel rearranges its structure so rapidly relative to the passage of ions through it that its structure can be assumed to be in equilibrium for its occupancy state at all times or, alternatively, when the channel's conformational structure is fixed (the electron cloud can rearrange instantaneously but not the atoms themselves). We don't know yet how much this picture of a channel affects our interpretation of selectivity. Some molecular models of the interaction energies between ions and ligands are completely static, such as a coulombic electrostatic model. Others (e.g., thermochemical models) contain implicit assumptions about time averaging of interaction energies. (The energy terms governing electron cloud and core rearrangements themselves have characteristic frequencies (*U–V, I–R,* microwave) which are fast compared to the usual electrical time scale).

Lauger has considered the possibility that channel proteins, like other proteins [72], are dynamic structures which undergo fluctuations, i.e., conformational changes, that can affect permeation. The conformational changes can, in this view, be influenced by the ions inside the channel. This concept introduces great complexities in theoretical analysis and may uncover serious flaws in previous interpretations of experimental data. The idea is, however, conceptually appealing and already has some verification in a biological channel (*see* below). We will restrict our discussion to points which may be relevant to selectivity.

One intriguing consequence of considering the dynamic properties of the interactions between an ion and the channel was suggested to us by Sally Krasne. Although we have previously argued that the ion-barrier and ion-well interactions are similar according to classical Rate Theory, the dwell time of an ion in a well will obviously tend to be much longer than that at the quasi-equilibrium transition state at a peak. This implies that the channel, and possibly the ion itself, has more time to rearrange itself in an ion-well interaction. Certain types of interactions (e.g. molecular, as opposed to electronic, polarizations or conformational changes) might thus be more likely to occur at wells than at peaks. It is also possible in this view that the selectivity of wells will have a greater tendency to show non-Eisenman sequences (*recall* Fig. 6). Other differences between peaks and wells are discussed below.

To reiterate, the time course of fluctuations in channel proteins may be fast, comparable, or slow by comparison with the time course of ion movement through a channel. For example, the speed of deformation vibrations in peptides are of the same order of magnitude as ion hopping [75]. Gating processes, on the other hand, which are responsible for the opening and closing of channels, are much slower. Lauger et al. [85] have shown for a Rate Theory model that although rapid fluctuations have no effect on the overall form of flux equations for permeation, the apparent energy levels of barriers and wells are influenced by the frequency of fluctuations and may therefore be difficult to interpret. Slower conformational changes cause fundamental alterations in the flux equations. In some cases a one-ion channel with fluctuating barriers has the properties of a multi-ion channel, in that the conductance *vs.* concentration relationship can have a maximum [85]. If such slow fluctuations approach the time scale of physiological measurements, then they could possibly be studied directly. A recent report by Sigworth [117] shows that open acetylcholine receptor channels produce excess current noise over background levels. He interpreted his data as a consequence of some fluctuations in the energy barriers for ions in the channel. His data were not consistent, for example, with transport noise of ions passing through the channel [82, 45], or with noise produced by a rapid gating process which interrupts current flow in an all-or-none fashion.

Some of the most fascinating work along this line has been the attempt to study ion movement under conditions where the fluctuations of the channel protein are on a similar time scale as ion

movements. The most convincing analyses have been molecular dynamics (MD) simulations, in which the behavior of an ion interacting with ligands along a channel wall is calculated by explicitly integrating the coupled Newtonian equations of motion [43, 44]. Such simulations, even for the simple models used, are very time consuming on a computer, and so far the presence of water has been neglected. The protein channel was modelled as a rigid, hexagonal helix with flexible dipoles (carbonyl groups) which extend into the axis of the channel. In the original study [44] the one-dimensional movement of a monovalent cation was restricted to the axis. However, its movement was dynamically coupled to the oscillatory movements of the dipoles. The interaction between the cation and the channel was determined by a combination of electrostatic and van der Waals forces. Depending on the physical arrangement of the dipoles, the apparent energy profile seen by the cation was a series of peaks and wells. The softness of the channel was allowed to vary in these simulations. A soft channel has slow vibrational frequencies of the carbonyl groups lining the channel; hard channels have faster vibrational frequencies. In a subsequent paper [43] the ion was only restricted to remain within the channel, but could move laterally from wall to wall. By examining the trajectories of the ions in detail Fischer and Brickmann [43] were able to show that in soft channels ions seemed to diffuse through the channel in a Brownian-like motion. In hard channels they hopped from site to site.

In spite of the simplicity of the models, several interesting results were obtained. For example, the calculated rate of ion flux through the channel was considerably larger than might be expected from the temperature dependence of the flux, which is usually considered to be a measure of activation enthalpy [44]. This can be thought of as due to a high activation entropy induced by the freedom of dipoles to rearrange in response to the permeating cation. The large entropy was shown to depend on the size of the cation, and this effect was primarily due to interactions between the cation and channel at energy minima [10]. These effects would be greater for a narrower pore. The size dependence of activation entropy can explain the fact that large, heavy ions (e.g., Cs) tend to move more rapidly through many channels than smaller, lighter ions (e.g., Li). This can be explained by the fact that smaller ions migrate more slowly through wells. The peaks, however, did not discriminate between ions according to size, but rather according to mass. This is another example of fundamental differences between wells and peaks. Such a relationship, i.e., large temperature dependence of current together with large single-channel conductance, has been observed in acetylcholine receptor channels [42, 64, 111], again suggesting a nonstatic view of the energy profile for ion movement through this channel.[16]

The MD simulations, although powerful, are quite cumbersome. A number of mean force models have also been attempted [84, 115]. These models have calculated average jump rates from site to site, using a variation of Rate Theory. The classical form of Rate Theory, which we have discussed earlier in this paper, considers the channel a rigid, static structure. However, it is possible to use the Rate Theory approach to calculate jump rates for ion movement in a more dynamic situation. Although this approach lacks the precise time information of MD simulations, it can provide insights about molecular interactions between ions and the channel that the classical Rate Theory models cannot. For example, Lauger [84] has calculated ion movements using microscopic parameters such as atomic coordinates, force constants, and intermolecular energy parameters for a system with relatively rapid fluctuations. Again using a helical channel with flexible dipolar ligands, in the absence of water, he was able to compare the energy profile for Cs and Li. He found that Li had much deeper wells than Cs, but a similar energy for the barriers. This again was due to the polarizing power of the smaller Li ion. Finally Lauger calculated the conductance of all of the alkali metal cations. Relative conductance depended strongly on temperature. The sequences at all temperatures were found to be polarizability sequences. Although these sequences, owing to the absence of hydration effects, are not strictly comparable to the selectivity sequences discussed earlier in the present paper, their non-monotonic dependence on ion radius also depends upon the presence of several energy terms having different dependences on cation size. The origin of these sequences seems to be analogous to the origin of the sequences observed for the melting points for the alkali halide crystals (*cf.* Pauling, [105], Fig. 13.8), which follow Eisenman sequences despite arising in a completely anhydrous system.[17]

[16] An alternative interpretation is that an ion releases waters of hydration at the top of an energy barrier (*cf.* [56]). The increased entropy of the water might be responsible for a net increase in activation entropy for the reaction [91]. This would also lead to a large temperature dependence of conductance.

[17] It is of interest that an Eisenman sequence is observed in Fischer and Brickmann's ([43], Fig. 6) plot of calculated site-to-site transition rates as a function of channel softness.

Brickmann and Fischer [10] have carried out a similar Rate Theory analysis of a channel having the same molecular properties as in their MD models. They have included the possibility for ions to move in all three dimensions. Their results were consistent with those obtained in the MD simulations, providing some test of the validity of this use of Rate Theory. Specifically the ion size-dependence of diffusion rate could be accounted for. Finally, Schroder [115], using a rather general procedure, constructs the Hamiltonian for a particular model where the ion is restricted to the axis of the channel, but its movements are coupled to the oscillatory movements of dipoles lining a channel with elastically bound ligands. He then deduces the transport properties, generalizing conventional Rate Theory somewhat, to produce a Mass Dependent Rate Theory. From this treatment he finds that the jump rate does not possess the local character it did with conventional Rate Theory, but instead depends upon the properties and behavior of all channel particles. He finds that the apparent entropy of activation in hopping over a barrier is temperature dependent, leading to a temperature dependent activation energy. This was also consistent with MD simulations.

Perhaps the greatest difficulty in interpreting this line of research is the absence of water in all of the calculations. Hopefully in future studies water will be considered as an important entity, both at the level where an ion enters a channel, and as a constituent within the channel [41].

We thank John Dani, Bertil Hille, and Sally Krasne for their perceptive and helpful comments on the manuscript and acknowledge the generous support of the National Science Foundation (PCM 76-20605) and the U.S. Public Health Service (GM 24749, NS 18608, and NS 00703), without which the work reported here could not have been accomplished.

References

1. Adams, D.J., Dwyer, T.M., Hille, B. 1980. *J. Gen. Physiol.* **75**:493–510
2. Adams, D.J., Nonner, W., Dwyer, T.M., Hille, B. 1981. *J. Gen. Physiol.* **78**:593–615
3. Armstrong, C.M. 1975. *In:* Membranes, A Series of Advances. G. Eiseman, editor. Vol. 3, pp. 325–358. Marcel Dekker, New York
4. Begenisich, T. 1979. *In:* Membrane Transport Processes. C.F. Stevens and R.W. Tsien, editors. Vol. 3, pp. 105–111. Raven Press, New York
5. Begenisich, T., Stevens, C.F. 1975. *Biophys. J.* **15**:843–846
6. Begenisich, T.B., Cahalan, M.D. 1980. *J. Physiol (London)* **307**:217–242
7. Begenisich, T.B., Cahalan, M.D. 1980. *J. Physiol. (London)* **307**:243–257
8. Bezanilla, F., Armstrong, C.M. 1972. *J. Gen. Physiol.* **60**:588–608
9. Boyle, P.J., Conway, E.J. 1941. *J. Physiol. (London).* **100**:163
10. Brickmann, J., Fischer, W. 1983. Entropy effects on the ion diffusion rate in transmembrane protein channels. *Biophys. Chem. (in press)*
11. Brown, K.M., Dennis, J.E. 1972. *Num. Math.* **18**:289–297
12. Bungenberg de Jong, H.G. 1949. *In:* Colloid Science. pp. 287. Elsevier, Amsterdam
13. Ciani, S. 1965. *Biophysik.* **2**:368–378
14. Ciani, S.M., Eisenman, G., Laprade, R., Szabo, G. 1973. *In:* Membranes, A Series of Advances. G. Eisenman, editor. Vol. 2, pp. 61–177. Marcel Dekker, New York
15. Colquhoun, D., Hawkes, A.G. 1981. *Proc. R. Soc. London B* **211**:205–235
16. Coronado, R., Miller, C. 1982. *J. Gen. Physiol.* **79**:529–547
17. Coronado, R., Rosenberg, R.L., Miller, C. 1980. *J. Gen. Physiol.* **76**:425–446
18. Dani, J.A., Levitt, D.G. 1981. *Biophys. J.* **35**:485–500
19. Diamond, J.M., Wright, E. 1969. *Annu. Rev. Physiol.* **31**:581–646
20. Dwyer, T.M., Adams, D.J., Hille, B. 1980. *J. Gen. Physiol.* **75**:469–492
21. Eberl, D.D. 1980. *Clays Clay Min.* **28**:161–172
22. Eigen, M., Winkler, R. 1970. *In:* The Neurosciences. F.O. Schmitt, editor. Vol. II, pp. 685–696. Rockefeller University Press, New York
23. Eisenman, G. 1961. *In:* Symposium on Membrane Transport and Metabolism. A. Kleinzeller and A. Kotyk, editors. pp. 163–179. Academic Press, New York
24. Eisenman, G. 1962. *Biophys. J.* **2 (2)**:259–323
25. Eisenman, G. 1965. *In:* Proc. XXIIIrd Int. Congr. *Physiol. Sci. (Tokyo)* **87**:489–506
26. Eisenman, G. 1969. *In:* Ion-Selective Electrodes. R.A. Durst, editor. pp. 1–56. National Bureau of Standards Special Publication 314
27. Eisenman, G. 1983. *In:* Mass Transfer and Kinetics on Ion Exchange. L. Liberti, editor. NATO Advanced Study Institute Series, Martinus Nijhoff Publ. *(in press)*
28. Eisenman, G., Conti, F. 1965. *J. Gen. Physiol.* **48 (2)**:65–73
29. Eisenman, G., Hagglund, J., Sandblom, J., Enos, B. 1980. *Uppsala J. Med. Sci.* **85**:247–257
30. Eisenman, G., Krasne, S. 1975. *In:* MTP International Review of Science, Biochemistry Series. C.F. Fox, editor. Vol. 2, pp. 27–59. Butterworths, London
31. Eisenman, G., Krasne, S., Ciani, S. 1975. *Ann. N.Y. Acad. Sci.* **264**:34–60
32. Eisenman, G., Krasne, S., Ciani, S. 1976. *In:* Ion and Enzyme Electrodes in Medicine and in Biology. M. Kessler, L. Clark, D. Lubbers, I. Silver, and W. Simon, editors. pp. 3–22. Urban and Schwarzenberg, Munich – Berlin – Vienna
33. Eisenman, G., Rudin, D.O., Casby, J.U. 1957*a*. *Science* **126**:831–834
34. Eisenman, G., Rudin, D.O., Casby, J.U. 1957*b*. *In:* 10th Annual Conference on Electrical Techniques in Medicine and Biology of the A.I.E.E., I.S.A., and I.R.E., Boston
35. Eisenman, G., Sandblom, J.P. 1983. *In:* Physical Chemistry of Transmembrane Motions. G. Spach, editor. pp. 329–347. Elsevier, Amsterdam
36. Eisenman, G., Sandblom, J., Hagglund, J. 1983. *In:* Structure and Function in Excitable Cells. W. Adelman, D. Chang, R. Leuchtag, and I. Tasaki, editors. Plenum, New York *(in press)*
37. Eisenman, G., Sandblom, J., Neher, E. 1977. *In:* Metal-Ligand Interactiions in Organic Chemistry and Biochemistry. Vol. 9, Part 2. B. Pullman and N. Goldblum, editors. pp. 1–36. Reidel, Dordrecht

38. Eisenman, G., Sandblom, J., Neher, E. 1978. *Biophys. J.* **22**:307–340
39. Eisenman, G., Szabo, G., Ciani, S., McLaughlin, S., Krasne, S. 1973. *Prog. Surf. Membr. Sci.* **6**:139–241
40. Eyring, H., Lumry, R., Woodbury, J.W. 1949. *Rec. Chem. Prog.* **10**:100–114
41. Finkelstein, A., Andersen, O.S. 1981. *J. Membrane Biol.* **59**:155–171
42. Fischbach, G.D., Lass, Y. 1978. *J. Physiol. (London)* **280**:527–536
43. Fischer, W., Brickmann, J. 1983. *In:* Physical Chemistry of Transmembrane Motions. G. Spach, editor. pp. 415–422. Elsevier Amsterdam
44. Fischer, W., Brickmann, J., Lauger, P. 1981. *Biophys. Chem.* **13**:105–116
45. Frehland, E., Stephan, W. 1979. *Biochim. Biophys. Acta* **553**:326–341
46. Gage, P.W., Helden, D.F. van 1979. *J. Physiol. (London)* **288**:509–528
47. Gay, L.A., Stanfield, P.R. 1978. *Nature (London)* **276**:169–170
48. Glasstone, S., Laudler, K.J., Eyring, H. 1941. The Theory of Rate Processes. McGraw-Hill, New York
49. Goldman, D. 1943. *J. Gen. Physiol.* **27**:37–60
50. Gorman, A.L.F., Woolum, J.C., Cornwall, M.D. 1982. *Biophys. J.* **38**:319–322
51. Grell, E., Funck, T., Eggers, F. 1975. *In:* Membranes, A Series of Advances. G. Eisenman, editor. Vol. 3, pp. 1–126. Marcel Dekker, New York
52. Gresh, N., Etchebest, C., Luz Rojas de la, O., Pullman, A. 1981. *Int. J. Quant. Chem.* **8**:109–116
53. Gresh, N., Pullman, A. 1982. A theoretical study of the interaction of nonactin with Na^+, and NH_4^+. *Int. J. Quant. Chem. (in press)*
54. Hille, B. 1971. *J. Gen. Physiol.* **58**:599–619
55. Hille, B. 1972. *J. Gen. Physiol.* **59**:637–658
55*a*. Hille, B. 1973. *J. Gen. Physiol.* **61**:669–686
56. Hille, B. 1975*a*. *In:* Membranes, A Series of Advances. G. Eisenman, editor. Vol. 3, pp. 255–323. Marcel Dekker, New York
57. Hille, B. 1975*b*. *J. Gen. Physiol.* **66**:535–560
58. Hille, B., Schwarz, W. 1978. *J. Gen. Physiol.* **72**:409–442
59. Hladky, S.B., Haydon, D.A. 1972. *Biochim. Biophys. Acta* **274**:294–312
60. Hladky, S.B., Urban, B.W., Haydon, D.A. 1979. *In:* Membrane Transport Processes. C.F. Stevens and R.W. Tsien, editors. Vol. 3, pp. 89–103. Raven Press, New York
61. Hober, R. 1905. *Pflugers Arch. Ges. Physiol.* **106**:599–635
62. Hodgkin, A.L., Katz, B. 1949. *J. Physiol. (London)* **108**:37–77
63. Hodgkin, A.L., Keynes, R.D. 1955. *J. Physiol. (London)* **128**:61–88
64. Hoffman, H.M., Dionne, V.E. 1982. *Biophys. J.* **37**:19*a*
65. Horn, R., Brodwick, M.S. 1980. *J. Gen. Physiol.* **75**:297–321
66. Horn, R., Brodwick, M.S., Dickey, W.D. 1980. *Science* **210**:205–207
67. Horn, R., Patlak, J., Stevens, C.J. 1981. *Biophys. J.* **36**:321–327
68. Horn, R., Stevens, C.F. 1980. *Comm. Mol. Cell. Biophys.* **1**:57–68
69. Huang, L-Y.M., Catterall, W.A., Ehrenstein, G. 1978. *J. Gen. Physiol.* **71**:397–410
70. Jack, J.J.B., Noble, D., Tsien, R.W. 1975. The Spread of Current in Excitable Cells. Clarendon Press, Oxford
71. Jenny, H. 1932. *J. Physiol. Chem.* **36**:2217–2258
72. Karplus, M., McCammon, J.A. 1981. *CRC Crit. Rev. Biochem.* **9**:293–349
73. Karreman, G., Eisenman, G. 1962. *Bull. Math. Biophys.* **24**:413–427
74. Kohler, H.-H., Heckmann, K. 1980. *J. Membr. Sci.* **6**:45–59
75. Koyama, Y., Shimanouchi, T. 1974. *In:* Peptides, Polypeptides and Proteins. E.R. Blout, F.A. Bovey, M. Goodman, and N. Lotan, editors. pp. 396–418. John Wiley, New York
76. Krasne, S. 1978. *In:* Physiology of Membrane Disorders. T.E. Andreoli, J.F. Hoffman, and D.D. Fanestil, editors. Ch. 12, pp. 217–241. Plenum Medical, New York
77. Krasne, S., Eisenman, G. 1973. *In:* Membranes, A Series of Advances. G. Eisenman, editor. Vol. 2, pp. 277–328. Marcel Dekker, New York
78. Krasner, S., Eisenman, G. 1976. *J. Membrane Biol.* **30**:1–44
79. Laprade, R., Ciani, S., Eisenman, G., Szabo, G. 1975. *In:* Membranes, A Series of Advances. G. Eisenman, editor. Vol. 3, pp. 127–214. Marcel Dekker, New York
80. Latorre, R., Miller, C. 1983. *J. Membrane Biol.* **71**:11–30
81. Lauger, P. 1973. *Biochim. Biophys. Acta* **311**:423–441
82. Lauger, P. 1979. *Biochim. Biophys. Acta* **557**:283–294
83. Lauger, P. 1980. *J. Membrane Biol.* **57**:163–178
84. Lauger, P. 1982. *Biophys. Chem.* **15**:89–100
85. Lauger, P., Stephan, W., Frehland, E. 1980. *Biochim. Biophys. Acta* **602**:167–180
86. Levitt, D.G. 1982. *Biophys. J.* **37**:575–587
87. Lewis, C. 1979. *J. Physiol. (London)* **286**:417–445
88. Lindley, B.D., Hoshiko, T. 1964 *J. Gen. Physiol.* **47**:749–771
89. Ling, G.N. 1952. *In:* Phosphorus Metabolism. W.D. McElroy and B. Glass, editors. Vol. II, pp. 748–795. Johns Hopkins, Baltimore
90. Ling, G.N. 1962. A Physical Theory of the Living State. Ginn (Blaisdell), Boston
91. Loftfield, R.B., Eigner, E.A., Pastuszyn, A., Lovgren, T.N.E., Jakubowski, H. 1980. *Proc. Natl. Acad. Sci. USA* **77**:3374–3378
92. Marchais, D., Marty, A. 1979. *J. Physiol. (London)* **297**:9–45
93. Marty, A. 1981. *Nature (London)* **291**:497–500
94. Mattock, G. 1961. pH Measurement and Titration. pp. 130–134. Heywood, London
95. McBride, D.W. 1981. Anomalous Mole Fraction Behavior, Momentary Block, and Lifetimes of Gramicidin A in Silver and Potassium Fluoride Solutions. Ph.D. Thesis, University of California, Los Angeles
96. Michaelis, L. 1925. *J. Gen. Physiol.* **8**:33–59
97. Miller, C. 1982*a*. *In:* Transport in Biological Membranes. R. Antolini, editor. pp. 99–108. Raven Press, New York
98. Miller, C. 1982*b*. *J. Gen. Physiol.* **79**:869–891
99. Morf, W.E. 1981. The Principles of Ion-Selective Electrodes and of Membrane Transport. Elsevier, Amsterdam
100. Mullins, L.J. 1959. *J. Gen. Physiol.* **42**:817–829
101. Mullins, L.J. 1975. *Biophys. J.* **15**:921–931
102. Myers, V.B., Haydon, D.A. 1972. *Biochim. Biophys. Acta* **274**:313–322
103. Neher, E., Steinbach, J.H. 1978. *J. Physiol. (London)* **277**:153–176
104. Pallotta, B.S., Magleby, K.L., Barrett, J.N. 1981. *Nature (London)* **293**:471–474
105. Pauling, L. 1960. The Nature of the Chemical Bond. (3rd. Ed.) Cornell University, Ithaca
106. Procopio, J., Andersen, O.S. 1979. *Biophys. J.* **25**:8*a*

107. Reichenberg, D. 1966. *In:* Ion Exchange, A Series of Advances. J.A. Marinsky, editor. Vol. 1, pp. 227–276. Marcel Dekker, New York
108. Reid, E.W. 1898. *In:* Textbook in Physiology. E.A. Schafer, editor. Young J. Pentland, Edinburgh
109. Reuter, H., Stevens, C.F. 1981. *J. Membrane Biol.* **57:**103–118
110. Ring, A., Sandblom, J. 1983. *J. Memb. Sci. (in press)*
111. Sachs, F., Lecar, H. 1977. *Biophys. J.* **17:**129–143
112. Sandblom, J., Eisenman, G., Hagglund, J.V. 1983. *J. Memb. Biol.* **71:**61–78
113. Sandblom, J., Eisenman, G., Neher, E. 1977. *J. Membrane Biol.* **31:**383–417
114. Schagina, L.V., Grinfeldt, A.E., Lev, A.A. 1978. *Nature (London)* **273:**243–245
115. Schroder, H. 1983. Rate theoretical analysis of ion transport in membrane channels with elastically bound ligands. *In:* Physical Chemistry of Transmembrane Motions. G. Spach, editor. pp. 425–436. Elsevier, Amsterdam
116. Sherry, H.S. 1969. *In:* Ion Exchange. J. Marinsky, editor. pp. 89–133. Marcel Dekker, New York
117. Sigworth, F.J. 1982. *Biophys. J.* **37:**309*a*
118. Simon, W., Morf, W.E. 1973. *In:* Membranes. A Series of Advances. G. Eisenman, editor. pp. 329–375. Marcel Dekker, New York
119. Swenson, R.P., Armstrong, C.M. 1981. *Nature (London)* **291:**427–429
120. Takeda, K., Barry, P.H., Gage, P.W. 1982. *Proc. R. Soc. London B.* **216:**225–251
121. Thomas, R.C., Meech, R.W. 1982. *Nature (London)* **299:**826–828
122. Truesdell, A.H., Christ, C.L. 1967. *In:* Glass Electrodes for Hydrogen and Other Cations. G. Eisenman, editor. Ch. 11, pp. 293–321. M. Dekker, New York
123. Urban, B.W., Hladky, S.B. 1979. *Biochim. Biophys. Acta* **554:**410–429
124. Urban, B.W., Hladky, S.B., Haydon, D.A. 1980. *Biochim. Biophys. Acta* **602:**331–354
125. Urry, D.W., Venkatachalam, C.M., Spisni, A., Bradley, R.J., Trapane, T.L., Prasad, K.U. 1980. *J. Membrane Biol.* **55:**29–51
126. Woodbury, J.W. 1971. *In:* Chemical Dynamics: Papers in Honor of Henry Eyring. J.O. Hirschfelder, editor. pp. 601–661. Wiley, New York
127. Woodhull, A.M. 1973. *J. Gen. Physiol.* **61:**687–708
128. Zwolinsky, B.J., Eyring, H., Reese, C.E. 1949. *J. Physiol. Colloid Chem.* **53:**1426–1453

Received 7 January 1983; revised 23 May 1983